

Hierarchy of correlations: Application to Green's functions and interacting topological phases

Álvaro Gómez-León

*Department of Physics and Astronomy and Pacific Institute of Theoretical Physics
University of British Columbia, 6224 Agricultural Rd., Vancouver, B.C., V6T 1Z1, Canada**

(Dated: July 21, 2016)

We study the many-body physics of different quantum systems using a hierarchy of correlations, which corresponds to a generalization of the $1/\mathcal{Z}$ hierarchy. The decoupling scheme obtained from this hierarchy is adapted to calculate double-time Green's functions, and due to its non-perturbative nature, we describe quantum phase transition and topological features characteristic of strongly correlated phases. As concrete examples we consider spinless fermions in a dimerized chain and in a honeycomb lattice. We present analytical results which are valid for any dimension and can be generalized to different types of interactions (e.g., long range interactions), which allows us to shed light on the effect of quantum correlations in a very systematic way. Furthermore, we show that this approach provides an efficient framework for the calculation of topological invariants in interacting systems.

Contents

I. Introduction	1
II. Hierarchy of correlations	2
III. Real space hierarchy	3
A. Uncorrelated solution	4
Self-consistency equations	5
B. Correlated solution	5
Self-consistency equations	6
IV. k Space hierarchy	7
A. Uncorrelated solution	9
B. Correlated solution	10
Self-consistency equations	10
V. Topological properties	11
VI. Conclusions	14
References	15
A. Correlated part of the 4-point function	16

I. INTRODUCTION

The study of quantum many-body systems is a very active research field, mainly due to the large number of fascinating effects that can be observed. The main reason for the large degree of complexity in these systems is the presence of non-local correlations between particles. The development of different methods to extract the relevant information for their description is then crucial, and an important source of progress and debate in the field. While many standard techniques such as diagrammatic, bosonization¹, dynamical mean field theory^{2,3}, etc, have been applied, it is not always clear how corre-

lations are treated in these approximations, and this can cause problems in the description of the system.

A very important feature of quantum many-body systems is the existence of quantum phase transitions (QPT)⁴. They describe a change in the many-body ground state properties of a quantum system when a physical parameter is tuned. Unlike classical phase transitions, which are driven by thermal fluctuations, QPT are driven by quantum fluctuations, and are strictly speaking, $T = 0$ phase transitions. The characterization of phase transitions has notably evolved, starting from the description of classical phase transitions by Ehrenfest, to the characterization and classification of order parameters by Landau⁵, or the modern dynamical mean field theories (not to mention the crucial renormalization group theory developed by Wilson⁶). Crucially, it has been shown that the non-analyticity of the transitions is ubiquitous in all these approaches, meaning that perturbative methods (in the sense of standard perturbation theory) are not generally enough for their description.

Another important feature of many-body systems, intensively studied in the last decade, is topological phase transitions (TPT)^{7,8}. In general, the topological phases cannot be characterized using an order parameter, which makes them different from the usual QPT, and one needs to calculate topological invariants. Furthermore, their bulk spectral properties cannot be differentiated from those of trivial phases, and only when looking at the boundary of the system, can one observe the physical differences due to the presence of edge modes. Although all the main properties and possible topological phases are well understood for the case of non-interacting systems⁹, the effect of interactions is still unclear and requires further studies. Nevertheless, huge progress has been made in the last years, and numerous phases with very interesting properties have been predicted¹⁰⁻¹⁶.

A very interesting method used to characterize magnetic systems -archetypal examples in the theory of quantum phase transition¹⁷- is the $1/\mathcal{Z}$ expansion, where \mathcal{Z} is the coordination number of the system^{18,19}. In this

case, one assumes that contributions from the interaction part of the Hamiltonian scale inversely proportional to \mathcal{Z} , providing a hierarchical expansion of the different statistical averages. From this very general argument, it is clear that the hierarchy will be accurate in high dimensional systems (where the coordination number is large), which is the reason why it has been mainly applied in the description of 3D materials. Studies of electronic and bosonic systems with itinerant particles have also been recently analyzed using this approach²⁰.

In this work we discuss the origin of the coordination number scaling, and show that it can be derived from the monogamy property of entanglement. This feature makes the $1/\mathcal{Z}$ expansion equivalent to an expansion in terms of spatial correlations, and their scaling allows to approximate the n -point functions. This connection allows us to generalize the hierarchy to \mathbf{k} space, and obtain a different scaling for \mathbf{k} space correlations. We show that for low dimensional systems it is more effective to study \mathbf{k} space correlations, as they provide a faster convergence for the hierarchy. We prove explicitly these results in a honeycomb lattice^{21–25} and in a dimerized 1D chain, both populated by spinless fermions. Finally, we take advantage of the non-perturbative nature of this approach to analyze the topological properties of the dimerized chain. We show that the hierarchy of correlations allows to extract the topological invariants beyond the non-interacting limit.

II. HIERARCHY OF CORRELATIONS

The conventional assumption of the $1/\mathcal{Z}$ hierarchy is that the interaction part of the Hamiltonian, proportional to V , scales as $1/\mathcal{Z}$, where \mathcal{Z} is the coordination number of the system. At first glance, this can be interpreted as an expansion in the interaction part of the Hamiltonian; however this is not the case, and the expansion is not done in terms of a small parameter, but rather in terms of decreasing contributions of correlations to the density matrix. Formally, we can derive the hierarchy as follows: Let us introduce the density matrix of a system ρ , and the reduced density matrix $\rho_{\mathbf{x}} = \text{Tr}_{\mathbf{x}}\{\rho\}$, where $\text{Tr}_{\mathbf{x}}\{\rho\}$ means trace over all degrees of freedom but \mathbf{x} (\mathbf{x} corresponds to a specific lattice site for the case of the $1/\mathcal{Z}$ hierarchy). If we consider the 2-point reduced density matrix $\rho_{\mathbf{x},\mathbf{y}} = \text{Tr}_{\mathbf{x},\mathbf{y}}\{\rho\}$, we can rewrite this quantity as follows:

$$\rho_{\mathbf{x},\mathbf{y}} = \rho_{\mathbf{x}}\rho_{\mathbf{y}} + \rho_{\mathbf{x},\mathbf{y}}^C \quad (1)$$

where $\rho_{\mathbf{x},\mathbf{y}}^C$ is just the difference between the 2-point density matrix, and the product of 1-point density matrices at each point $\rho_{\mathbf{x}}\rho_{\mathbf{y}}$ (i.e., $\rho_{\mathbf{x},\mathbf{y}}^C$ contains the correlations between the two sites). If we assume the scaling $\rho_{\mathbf{x},\mathbf{y}}^C \sim 1/\mathcal{Z}$ (this is motivated in terms of the entanglement monogamy in the next paragraph), we find that the different statistical averages can be separated into their

uncorrelated part and contributions due to correlations, which decay with different inverse powers of the coordination number \mathcal{Z} . This defines the $1/\mathcal{Z}$ hierarchy.

Clearly one needs to justify the scaling $\rho_{\mathbf{x},\mathbf{y}}^C \sim \mathcal{Z}^{-1}$, and prove that the scaling $\rho_{\mathbf{x},\mathbf{y}}^C \sim \mathcal{Z}^{-1}$ implies $V \sim \mathcal{Z}^{-1}$ for the interaction term (which also proves the equivalence between the \mathcal{Z}^{-1} hierarchy and a hierarchy of correlations). To the question: Why is the scaling of correlations inversely proportional to the coordination number of the lattice?, one can argue that it must be related with the monogamy property of entanglement²⁶: The monogamy of entanglement states that a fully correlated state of particles cannot be entangled with an extra particle, unless the entanglement between the initial set is reduced. Let us apply this principle to a simple example: Consider Fig.1, where we have a simple square lattice populated by spinless fermions. For simplicity, we assume that they can only hop and interact with their nearest neighbors. Then, a simple Hamiltonian describing the system would be:

$$H = - \sum_{\langle \mathbf{x},\mathbf{y} \rangle} t_{\mathbf{x},\mathbf{y}} (f_{\mathbf{y}}^{\dagger} f_{\mathbf{x}} + f_{\mathbf{x}}^{\dagger} f_{\mathbf{y}}) + \sum_{\langle \mathbf{x},\mathbf{y} \rangle} V_{\mathbf{x},\mathbf{y}} n_{\mathbf{x}} n_{\mathbf{y}} \quad (2)$$

where $n_{\mathbf{x}} = f_{\mathbf{x}}^{\dagger} f_{\mathbf{x}}$ is the number of particles at site \mathbf{x} , $t_{\mathbf{x},\mathbf{y}}$ is the hopping between sites and $V_{\mathbf{x},\mathbf{y}}$ corresponds to the interaction between particles. In this representation, operators are defined at different points of the lattice, and the hopping as well as the interaction create correlations between sites, because their value depends on the relative distance between pairs of points. This is what we define as non-local terms of the Hamiltonian.

Let us calculate the time evolution of the time-ordered 2-point function $G_{\mathbf{z},\mathbf{z}}^T(t,t') = -i\langle f_{\mathbf{z}}(t), f_{\mathbf{z}}^{\dagger}(t') \rangle_T$ using the Heisenberg's equation of motion, which corresponds to the propagation of a particle excitation to and from site \mathbf{z} (i.e., is proportional to $\rho_{\mathbf{z}}$):

$$\begin{aligned} \partial_t G_{\mathbf{z},\mathbf{z}}^T(t,t') &= -i\delta(t-t') + 2i \sum_{\mathbf{x} \neq \mathbf{z}} t_{\mathbf{z},\mathbf{x}} G_{\mathbf{x},\mathbf{z}}^T(t,t') \\ &\quad - 2i \sum_{\mathbf{x} \neq \mathbf{z}} V_{\mathbf{z},\mathbf{x}} G_{\mathbf{x}\mathbf{x}\mathbf{z},\mathbf{z}}^T(t,t') \end{aligned} \quad (3)$$

where we have defined $G_{\mathbf{x}\mathbf{x}\mathbf{z},\mathbf{z}}^T(t,t') = -i\langle n_{\mathbf{x}}(t) f_{\mathbf{z}}(t), f_{\mathbf{z}}^{\dagger}(t') \rangle_T$. As the Green's function is calculated with respect to the density matrix ρ , we can use the decomposition in terms of correlations (Eq.1):

$$\begin{aligned} \partial_t G_{\mathbf{z},\mathbf{z}}^T(t,t') &= -i\delta(t-t') + 2i \sum_{\mathbf{x} \neq \mathbf{z}} t_{\mathbf{z},\mathbf{x}} \mathcal{G}_{\mathbf{x},\mathbf{z}}^T(t,t') \\ &\quad - 2i \sum_{\mathbf{x} \neq \mathbf{z}} V_{\mathbf{z},\mathbf{x}} [\langle n_{\mathbf{x}} \rangle \mathcal{G}_{\mathbf{z},\mathbf{z}}^T(t,t') + \mathcal{G}_{\mathbf{x}\mathbf{x}\mathbf{z},\mathbf{z}}^T(t,t')] \end{aligned} \quad (4)$$

where \mathcal{G} denotes the statistical average with respect to the correlated part of the density matrix $\rho_{\mathbf{x},\mathbf{z}}^C$. If the Hamiltonian only contains local contributions, we would

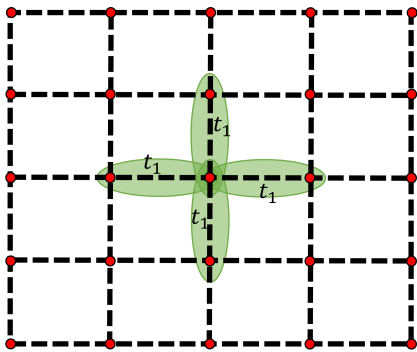


Figure 1: Representation of a particle in the central site of a square lattice. Due to non-local terms of the Hamiltonian (either nearest neighbor hopping t_1 or interaction V_1), the particle becomes correlated with the neighboring sites. The importance of these correlations is characterized by $\rho_{\mathbf{x},\mathbf{y}}^C$, being \mathbf{x},\mathbf{y} nearest neighbors. If the state is strongly correlated, $\rho_{\mathbf{x},\mathbf{y}}^C$ has reached a maximum value, and the entanglement with an extra site requires that $\rho_{\mathbf{x},\mathbf{y}}^C$ must decrease as $1/\mathcal{Z}$.

not find terms proportional to \mathcal{G} , as correlations would not propagate between different points of the lattice. However, the presence of these terms induce correlations between modes, proportional to the correlated part of the density matrix $\rho_{\mathbf{z},\mathbf{x}}^C$, and the possibility of collective excitations. If we assume that the resulting state between the particle excitation at site \mathbf{z} and its nearest neighbors is a strongly correlated one, this implies that $\rho_{\mathbf{z},\mathbf{x}}^C$ has reached a maximum value. Therefore, due to the monogamy property of entanglement, a change in the lattice including an extra nearest neighbor, would decrease $\rho_{\mathbf{z},\mathbf{x}}^C$ as \mathcal{Z}^{-1} . This analysis shows that the \mathcal{Z}^{-1} scaling of correlations follows directly from the monogamy of entanglement, if the system is strongly correlated.

Finally, once we have physically motivated the scaling $\rho_{\mathbf{z},\mathbf{x}}^C \sim \mathcal{Z}^{-1}$, we just need to relate the scaling of correlations with the physical parameters of the Hamiltonian. This can be easily done by direct calculation of the equation of motion for $\rho_{\mathbf{z},\mathbf{x}}^C$ ²⁰. One finds that in general, to lowest order in correlations, $\rho_{\mathbf{z},\mathbf{x}}^C$ turns out to be proportional to the non-local terms of the Hamiltonian t or V , times the product of the local density matrices $\rho_{\mathbf{x}}\rho_{\mathbf{z}}$. This implies that the non-local terms of the Hamiltonian must scale as $V, t \sim \mathcal{Z}^{-1}$. It is important to differentiate the meaning of the scaling \mathcal{Z}^{-1} from the actual value of the interaction/hopping, which is fixed when the model is defined. The meaning is that contributions to the statistical averages due to entanglement between modes is reduced as \mathcal{Z}^{-1} , and not that interactions become weaker as the coordination number increases. To stress this feature, the \mathcal{Z}^{-1} scaling is not directly incorporated in the Hamiltonian.

In summary, we have shown that the monogamy property of entanglement and the assumption of a strongly correlated state, naturally lead to the $1/\mathcal{Z}$ scaling of correlations and of non-local terms in the Hamiltonian. Fur-

thermore, as spatial correlations can be extremely different from the ones in \mathbf{k} space, we will explore these two different possibilities in the next sections and compare their scaling properties for different models³⁸.

III. REAL SPACE HIERARCHY

As we discussed in the previous section, the hierarchy of correlations can be established for different representations of the Hamiltonian. In position space, correlations between different points are created due to the non-local terms of the Hamiltonian. Furthermore, their scaling is proportional to the inverse of the coordination number \mathcal{Z} . Here we study the position space representation of the hierarchy, for a system of spinless fermions in a lattice with sub-lattice symmetry. The Hamiltonian can be written as:

$$H = - \sum_{\mathbf{x},\mathbf{x}'} \sum_{\sigma,\sigma'} \left(J_{\mathbf{x},\mathbf{x}'}^{\sigma,\sigma'} f_{\mathbf{x},\sigma}^\dagger f_{\mathbf{x}',\sigma'} + \text{h.c.} \right) \quad (5)$$

$$- \mu \sum_{\mathbf{x},\sigma} n_{\mathbf{x},\sigma} + \sum_{\mathbf{x},\mathbf{x}'} \sum_{\sigma,\sigma'} V_{\mathbf{x},\mathbf{x}'}^{\sigma,\sigma'} n_{\mathbf{x},\sigma} n_{\mathbf{x}',\sigma'}$$

where $f_{\mathbf{x},\sigma}^\dagger$ creates a fermion at position \mathbf{x} in sub-lattice σ (the sub-index σ can characterize other internal degrees of freedom as well), and $n_{\mathbf{x},\sigma} = f_{\mathbf{x},\sigma}^\dagger f_{\mathbf{x},\sigma}$ is the number of particles operator. This Hamiltonian contains a hopping term $J_{\mathbf{x},\mathbf{x}'}^{\sigma,\sigma'}$, a chemical potential μ that fixes the number of particles in the lattice, and a density-density interaction between the particles $V_{\mathbf{x},\mathbf{x}'}^{\sigma,\sigma'}$.

The numerical calculations in this work are particularized for a dimerized chain and a honeycomb lattice. For simplicity of our analysis we restrict the models to nearest neighbors, although the analytical results are valid for arbitrary number of neighbors interaction. We comment that the use of short-range interactions for the honeycomb lattice corresponds to a crude approximation of the real system due to the vanishing density of states at zero filling. However, it is also a very interesting approximation to understand the nature of phase transitions in 2D models. The hopping and interaction terms are:

- **Dimerized chain:** $J_{\mathbf{x},\mathbf{x}'}^{\sigma,\sigma'} = \delta_{\sigma',\bar{\sigma}} (t_1 \delta_{x,x'} + t_1' \delta_{x,x'-a})$ and $V_{\mathbf{x},\mathbf{x}'}^{\sigma,\sigma'} = V_1 \delta_{\sigma',\bar{\sigma}} (\delta_{x,x'} + \delta_{x,x'-a}) + V_2 \delta_{\sigma',\sigma} \delta_{x,x'-a}$, where for simplicity we have assumed that the interaction is symmetric between the sub-lattices, a is the length of the unit lattice vector and $\bar{\sigma} = -\sigma$.
- **Honeycomb lattice:** $J_{\mathbf{x},\mathbf{x}'}^{\sigma,\sigma'} = t_1 \delta_{\sigma',\bar{\sigma}} \sum_i \delta_{\mathbf{x},\mathbf{x}'+\mathbf{a}_i}$ and $V_{\mathbf{x},\mathbf{x}'}^{\sigma,\sigma'} = V_1 \delta_{\sigma',\bar{\sigma}} \sum_i \delta_{\mathbf{x},\mathbf{x}'+\mathbf{a}_i} + V_2 \delta_{\sigma',\sigma} \sum_i \delta_{\mathbf{x},\mathbf{x}'+\mathbf{b}_i}$, where $\mathbf{a}_{i=1,2,3}$ ($\mathbf{b}_{i=1,\dots,6}$) label the lattice vectors connecting the different nearest (next nearest) neighbors in the honeycomb lattice.

For the characterization of the physical properties we define a set of double time Green's functions:

$$G_{\mathbf{y},\mathbf{y}'}^{\alpha,\beta}(t,t') = -i\langle\langle f_{\mathbf{y},\alpha}(t); f_{\mathbf{y}',\beta}^\dagger(t') \rangle\rangle \quad (6)$$

where $\langle\langle \dots; \dots \rangle\rangle = \text{Tr}\{\rho \dots\}$ corresponds to the statistical average with respect to the density matrix ρ , for the advanced/retarded/time ordered Green's function (they all fulfill the same equation of motion, but with different boundary conditions). We assume that the system is in thermal equilibrium, and then the statistical average is calculated with respect to the thermal density matrix $\rho = e^{-\beta H}$. If we make use of the Heisenberg's equation of motion, and the fact that the system is in thermodynamic equilibrium, we find that the 2-point Green's function satisfies:

$$\begin{aligned} (\omega + \mu) G_{\mathbf{y},\mathbf{y}'}^{\alpha,\beta}(\omega) &= \frac{\delta_{\mathbf{y},\mathbf{y}'} \delta_{\alpha,\beta}}{2\pi} - 2 \sum_{\sigma,\mathbf{x}} J_{\mathbf{y},\mathbf{x}}^{\alpha,\sigma} G_{\mathbf{x},\mathbf{y}'}^{\sigma,\beta}(\omega) \\ &+ 2 \sum_{\sigma,\mathbf{x}} V_{\mathbf{y},\mathbf{x}}^{\alpha,\sigma} G_{\mathbf{x}\mathbf{x}\mathbf{y},\mathbf{y}'}^{\sigma\sigma\alpha,\beta}(\omega) \end{aligned} \quad (7)$$

where we have introduced the 4-point function $G_{\mathbf{x}\mathbf{x}\mathbf{y},\mathbf{y}'}^{\sigma\sigma\alpha,\beta}(\omega) \equiv -i\langle\langle f_{\mathbf{x},\sigma}^\dagger f_{\mathbf{x},\sigma} f_{\mathbf{y},\alpha} f_{\mathbf{y}',\beta}^\dagger \rangle\rangle$.

Eq.7 corresponds to the general expression for the equation of motion of the 2-point Green's function, which couples to higher n -point Green's functions and creates correlations between modes. The different approaches to find a solution to Eq.7 consist in different decoupling schemes to separate the higher n -point Green's functions into lower ones. As anticipated, in this work we make use of the hierarchy of correlations.

Before we continue, we comment on the hierarchy of correlations when couplings beyond nearest neighbors are included. Although we have derived the hierarchy for the simple case of nearest neighbors only, we can generalize the result to arbitrary neighbors: We can always decompose a general interaction into different contributions according to the lattice symmetries, e.g., $V_\delta^{\alpha,\sigma} = V_N^{\alpha,\sigma} + V_{NN}^{\alpha,\sigma} + \dots$, where N refers to nearest neighbors, NN to next nearest neighbors, etc. Each of these components generates a hierarchy of correlations with scaling proportional to $1/\mathcal{Z}_N$ for nearest neighbors, $1/\mathcal{Z}_{NN}$ for next nearest neighbors, etc. The idea is to find a lower bound for the scaling, where $V_i/\mathcal{Z}_i < V_j/\mathcal{Z}_j$ for all $i \neq j$. In this work we assume that the lower bound to the scaling is given by \mathcal{Z} , i.e., is a short range interaction in the sense $V_N/\mathcal{Z}_N < V_{NN}/\mathcal{Z}_{NN} < \dots$. This directly applies to the case of a dimerized chain, as the hopping to nearest neighbors can be separated in two different contributions. For simplicity we consider $t_1 \simeq t'_1$, which assumes a unique scaling for both bonds, but one could also define the lower bound for the hierarchy in terms of the two hoppings.

Finally, we expect that this hierarchy should be able to predict phases with enlarged unit cells due to interactions²³⁻²⁵. Although this is not discussed in the present work, we think that for higher orders of the hierarchy, Green's functions with different \mathbf{k} vectors will

couple in the equation of motion, and could predict the transition to phases with enlarged unit cells.

A. Uncorrelated solution

As we are dealing with a hierarchy of equations, we must systematically solve for the different $1/\mathcal{Z}$ orders. Here we first find the lowest order solutions for the Green's functions, i.e., when spatial correlations are neglected. If we expand Eq.7 in correlations, and neglect terms of order $1/\mathcal{Z}$ or higher, we find:

$$(\omega + \mu) g_{\mathbf{y},\mathbf{y}'}^{\alpha,\beta} = \frac{\delta_{\alpha,\beta}}{2\pi} + 2 \sum_{\sigma,\mathbf{x} \neq \mathbf{y}} \bar{n}_{\mathbf{x},\sigma} V_{\mathbf{y},\mathbf{x}}^{\alpha,\sigma} g_{\mathbf{y},\mathbf{y}'}^{\alpha,\beta} \quad (8)$$

where $g_{\mathbf{y},\mathbf{y}'}^{\alpha,\beta}$ denotes the uncorrelated Green's function (neglecting $1/\mathcal{Z}$ corrections), the $1/\mathcal{Z}$ factor in $V_{\mathbf{y},\mathbf{x}}^{\alpha,\sigma}$ is compensated by the sum over \mathbf{x} , and $\bar{n}_{\mathbf{x},\sigma} = \langle f_{\mathbf{x},\sigma}^\dagger f_{\mathbf{x},\sigma} \rangle_0$ corresponds to the uncorrelated local density of particles at site \mathbf{x} (we use the sub-index 0 to indicate that all correlations are neglected in the statistical average). Note that the equation of motion is similar to what is expected for a mean field theory in the strong coupling limit. As one would expect, the off-diagonal Green functions vanish, as they are proportional to $\rho_{\mathbf{y},\mathbf{y}'}^C$. The solution to Eq.8 is easily obtained:

$$g_{\mathbf{y},\mathbf{y}'}^{\alpha,\beta} = \frac{\delta_{\alpha,\beta}}{2\pi \left(\omega + \mu - 2 \sum_{\sigma,\mathbf{x}} \bar{n}_{\mathbf{x},\sigma} V_{\mathbf{y},\mathbf{x}}^{\alpha,\sigma} \right)} \quad (9)$$

where we have included the term $\bar{n}_{\mathbf{y},\sigma} V_{\mathbf{y},\mathbf{y}}^{\alpha,\sigma}$ in the sum, in order to simplify the expression (this term does not change the result, as it is of order $1/\mathcal{Z}$). Importantly, one must deal with the sum in the denominator, and in general, it could depend on long range interactions or on complicated local density distributions. One simple approximation is to assume that the number of particles in each sub-lattice is spatially homogeneous, i.e., we assume that $\langle f_{\mathbf{x},\sigma}^\dagger f_{\mathbf{x},\sigma} \rangle_0 = \bar{n}_\sigma = \sum_{\mathbf{x}} \bar{n}_{\mathbf{x},\sigma} / N$ is \mathbf{x} independent. In this case, the solution reduces to:

$$g_{\mathbf{y},\mathbf{y}'}^{\alpha,\beta} = \frac{\delta_{\alpha,\beta}}{2\pi(\omega - \omega_{0,\alpha})} \quad (10)$$

where $V_{\mathbf{q}}^{\alpha,\sigma} = \sum_{\delta} V_\delta^{\alpha,\sigma} e^{-i\mathbf{q}\delta}$ is the Fourier transform of the interaction potential and $\omega_{0,\alpha} = 2 \sum_{\sigma} \bar{n}_\sigma V_0^{\alpha,\sigma} - \mu$. This approximation is a reasonable one, as when correlations are neglected, all particles couple to an average field.

At this level of approximation, the structure of the Green's function exhibits a single pole at $\omega_{0,\alpha}$, which is proportional to the electron-electron interaction and the density of particles in each sub-lattice. This means that excitations correspond to adding or removing a particle, which couples to a charged background. Nevertheless, we do not know the density of particles in each sub-lattice $n_{\bar{\alpha}}$, and for a complete solution we must determine this

value self-consistently. This is done in the next subsection. Finally, we Fourier transform the previous equation of motion to \mathbf{k} space, as we will make use of the Green's function in Fourier space in the next sections. The solution is simply:

$$g_{\mathbf{k}}^{\alpha,\beta} = \frac{N\delta_{\alpha,\beta}\delta(\mathbf{k})}{2\pi(\omega - \omega_{0,\alpha})} \quad (11)$$

where once again, we have assumed that the average number of particles is spatially homogeneous in each sub-lattice: $\langle f_{\mathbf{x},\sigma}^\dagger f_{\mathbf{x},\sigma} \rangle_0^{\mathbf{q}} = N\bar{n}_\sigma\delta(\mathbf{q})$. Note that we use the superscript \mathbf{q} to indicate the Fourier transformed of the statistical average.

Self-consistency equations

In order to find the physical properties of the system, we must determine the different statistical averages by means of self-consistently equations. This can be done using the next expression, which relates the double-time Green's function with the statistical average²⁷:

$$\langle f_{\mathbf{y},\beta}^\dagger f_{\mathbf{y},\alpha} \rangle_0 = i \int \frac{g_{\mathbf{y},\mathbf{y}}^{\alpha,\beta}(\omega + i\epsilon) - g_{\mathbf{y},\mathbf{y}}^{\alpha,\beta}(\omega - i\epsilon)}{e^{\beta\omega} + 1} d\omega \quad (12)$$

Then, if we make use of the uncorrelated solutions found in Eq.11, the average number of particles is:

$$\langle f_{\mathbf{y},\beta}^\dagger f_{\mathbf{y},\alpha} \rangle_0^{\mathbf{k}} = N \frac{\delta_{\alpha,\beta}\delta(\mathbf{k})}{e^{\beta\omega_{0,\alpha}} + 1} \quad (13)$$

Importantly, this expression depends on the chemical potential μ and we need an extra equation for the solution. As μ is related with the number of particles in the system, the extra equation can be obtained from fixing the total number of particles:

$$N \sum_{\alpha} \bar{n}_{\alpha} = \sum_{\mathbf{x},\alpha} \langle f_{\mathbf{x},\alpha}^\dagger f_{\mathbf{x},\alpha} \rangle \quad (14)$$

where \bar{n}_{α} is the average number of particles in each sub-lattice:

$$\bar{n}_{\alpha} = \frac{1}{e^{\beta\omega_{0,\alpha}} + 1} \quad (15)$$

Now consider the case of a system with \mathbb{Z}_2 sub-lattice symmetry (as the honeycomb lattice or the dimerized

chain) at half filling. We obtain a system of three coupled equations:

$$\bar{n}_{\pm} = \frac{1}{e^{\beta\omega_{0,\pm}} + 1}, \quad \bar{n}_{+} + \bar{n}_{-} = 1 \quad (16)$$

with three unknown quantities (\bar{n}_{\pm} and μ). We find that the system of equations has a temperature independent solution for $\mu = V_0^{+,+} + V_0^{+,-}$, and that the number of particles is:

$$\bar{n}_{\pm} = \frac{1}{e^{\pm\beta x \delta V_0} + 1} \quad (17)$$

where $\delta V_0 = V_0^{+,+} - V_0^{-,+}$, and $x = \bar{n}_{+} - \bar{n}_{-}$ is the asymmetry factor. As the self-consistency equation for the asymmetry factor can be determined as well, we find:

$$x = -\tanh\left(\frac{\beta x \delta V_0}{2}\right) \quad (18)$$

Clearly the solution $x = 0$ is always valid, corresponding to a homogeneous charge distribution on the lattice. In the homogeneous charge phase (HCP) the particles are equally distributed between the two sub-lattices and $\bar{n}_{\alpha} = 1/2$. In addition, when nearest neighbor interaction dominates over next nearest neighbor ($\delta V_0 < 0$), $x \neq 0$ is also a solution with critical temperature given by $T_c = -\delta V_0$ (in units of the Boltzmann's constant k_B). In this case a charge density wave (CDW) phase forms for temperatures lower than the critical temperature. Note that when the system is at $T = 0$ this means that the CDW phase exists for any $V_1 > 0$. Thus, when correlations are neglected, the statistical averages reveal an insulating Mott phase with inhomogeneous charge distribution between the two sub-lattices. Interestingly, the solution neglecting correlations coincides with the strong coupling limit of a mean field theory.

B. Correlated solution

We now consider the full equation of motion for the Green's function (Eq.7), and include correlations up to $1/Z$ order using the expansion in correlations:

$$G_{\mathbf{x}\mathbf{y},\mathbf{y}'}^{\sigma\sigma\alpha,\beta} = \bar{n}_{\mathbf{x},\sigma} G_{\mathbf{y},\mathbf{y}'}^{\alpha,\beta} + G_{\mathbf{x}\mathbf{y},\mathbf{y}'}^{\sigma\sigma\alpha,\beta} \quad (19)$$

We find the next equations of motion:

$$\begin{aligned} \left(\omega + \mu - 2 \sum_{\sigma,\mathbf{x} \neq \mathbf{y},\mathbf{y}'} \bar{n}_{\mathbf{x},\sigma} V_{\mathbf{y},\mathbf{x}}^{\alpha,\sigma} \right) G_{\mathbf{y},\mathbf{y}'}^{\alpha,\beta} &= \frac{\delta_{\alpha,\beta}}{2\pi} - 2 \sum_{\sigma,\mathbf{x} \neq \mathbf{y}} J_{\mathbf{y},\mathbf{x}}^{\alpha,\sigma} G_{\mathbf{x},\mathbf{y}}^{\sigma,\beta} - 2 \sum_{\sigma} J_{\mathbf{y},\mathbf{y}'}^{\alpha,\sigma} g_{\mathbf{y},\mathbf{y}'}^{\sigma,\beta} \\ &+ 2 \sum_{\sigma,\mathbf{x} \neq \mathbf{y}} V_{\mathbf{y},\mathbf{x}}^{\alpha,\sigma} G_{\mathbf{x}\mathbf{y},\mathbf{y}'}^{\sigma\sigma\alpha,\beta} + 2 \sum_{\sigma} V_{\mathbf{y},\mathbf{y}'}^{\alpha,\sigma} g_{\mathbf{y}\mathbf{y},\mathbf{y}'}^{\sigma\sigma\alpha,\beta} \end{aligned} \quad (20)$$

$$\left(\omega + \mu - 2 \sum_{\sigma, \mathbf{x} \neq \mathbf{y}, \mathbf{y}'} \bar{n}_{\mathbf{x}, \sigma} V_{\mathbf{y}, \mathbf{x}}^{\alpha, \sigma} \right) \mathcal{G}_{\mathbf{y}, \mathbf{y}'}^{\alpha, \beta} = -2 \sum_{\sigma, \mathbf{x} \neq \mathbf{y}'} J_{\mathbf{y}, \mathbf{x}}^{\alpha, \sigma} \mathcal{G}_{\mathbf{x}, \mathbf{y}'}^{\sigma, \beta} - 2 \sum_{\sigma} J_{\mathbf{y}, \mathbf{y}'}^{\alpha, \sigma} g_{\mathbf{y}, \mathbf{y}'}^{\sigma, \beta} \quad (21)$$

where we have separated diagonal ($\mathbf{y} = \mathbf{y}'$) and off-diagonal ($\mathbf{y} \neq \mathbf{y}'$) Green's functions due to their different scaling properties. We remind the reader that the diagonal Green's function $G_{\mathbf{y}, \mathbf{y}}^{\alpha, \beta}$ contains terms of order 1 and $1/\mathcal{Z}$, $g_{\mathbf{y}, \mathbf{y}, \mathbf{y}}^{\sigma \sigma \alpha, \beta} \sim \mathcal{O}(1)$ corresponds to the uncorrelated part of the 4-point Green's function, and $\mathcal{G} \sim \mathcal{O}(1/\mathcal{Z})$ corresponds to the correlated part of the Green's function.

Eq.20 contains contributions from the 4-point Green's functions. For their calculation, we obtain the equation of motion and expand the higher n -point Green's functions in correlations. Neglecting all correlations we find that the uncorrelated 4-point function is:

$$g_{\mathbf{y}, \mathbf{y}, \mathbf{y}}^{\sigma \sigma \alpha, \beta} = \langle f_{\mathbf{y}, \sigma}^{\dagger} f_{\mathbf{y}, \sigma} \rangle_0 g_{\mathbf{y}, \mathbf{y}}^{\alpha, \beta} - \langle f_{\mathbf{y}, \sigma}^{\dagger} f_{\mathbf{y}, \alpha} \rangle_0 g_{\mathbf{y}, \mathbf{y}}^{\sigma, \beta} \quad (22)$$

which turns out to be equivalent to use Wick's theorem. Note that the pole structure is unchanged, as one would not expect new quasi-particles for the description of the system in absence of correlations. In addition, we have found that the expression for the 4-point function can be written in terms of 2-point functions, and can be used to simplify Eq.20:

$$(\omega - \omega_{0, \alpha}) G_{\mathbf{y}, \mathbf{y}}^{\alpha, \beta} = \frac{\delta_{\alpha, \beta}}{2\pi} + 2 \sum_{\sigma, \mathbf{x} \neq \mathbf{y}} V_{\mathbf{y}, \mathbf{x}}^{\alpha, \sigma} \mathcal{G}_{\mathbf{x}, \mathbf{y}}^{\sigma \sigma \alpha, \beta} \quad (23)$$

$$- 2 \sum_{\sigma} \left(J_{\mathbf{y}, \mathbf{y}}^{\alpha, \sigma} g_{\mathbf{y}, \mathbf{y}}^{\sigma, \beta} + \sum_{\mathbf{x} \neq \mathbf{y}} J_{\mathbf{y}, \mathbf{x}}^{\alpha, \sigma} \mathcal{G}_{\mathbf{x}, \mathbf{y}}^{\sigma, \beta} \right)$$

where we have absorbed the first term of Eq.22 into $G_{\mathbf{y}, \mathbf{y}'}^{\alpha, \beta} \sum_{\mathbf{x} \neq \mathbf{y}, \mathbf{y}'} \bar{n}_{\mathbf{x}, \sigma} V_{\mathbf{y}, \mathbf{x}}^{\alpha, \sigma}$, and used $\langle f_{\mathbf{y}, \sigma}^{\dagger} f_{\mathbf{y}, \alpha} \rangle_0 \propto \delta_{\sigma, \alpha}$. The Green's functions $\mathcal{G}_{\mathbf{x}, \mathbf{y}'}^{\sigma, \beta}$ and $\mathcal{G}_{\mathbf{x}, \mathbf{y}}^{\sigma \sigma \alpha, \beta}$, which are proportional to the correlated part of the density matrix, are calculated from their equation of motion. We find next pair of equations, which importantly, are decoupled from Eq.23:

$$(\omega - \omega_{0, \alpha}) \mathcal{G}_{\mathbf{k}, \mathbf{k}'}^{\alpha, \beta} = -2J_{\mathbf{k}}^{\alpha, \beta} g_{\mathbf{k}+\mathbf{k}'}^{\beta, \beta} - 2J_{\mathbf{k}}^{\alpha, \bar{\alpha}} \mathcal{G}_{\mathbf{k}, \mathbf{k}'}^{\bar{\alpha}, \beta} \quad (24)$$

$$(\omega - \omega_{0, \alpha}) \mathcal{G}_{\mathbf{z}, \mathbf{z}, \mathbf{y}}^{\sigma \sigma \alpha, \beta} = 2\bar{n}_{\sigma} (1 - \bar{n}_{\sigma}) g_{\mathbf{y}, \mathbf{y}}^{\alpha, \beta} V_{\mathbf{y}, \mathbf{z}}^{\alpha, \sigma} \quad (25)$$

$$+ 2g_{\mathbf{y}, \mathbf{y}}^{\alpha, \beta} \sum_{\sigma', \mathbf{x} \neq \mathbf{y}, \mathbf{z}} V_{\mathbf{y}, \mathbf{x}}^{\alpha, \sigma'} \langle n_{\mathbf{z}, \sigma} n_{\mathbf{x}, \sigma'} \rangle_C$$

being $\langle n_{\mathbf{z}, \sigma} n_{\mathbf{x}, \sigma'} \rangle_C = \langle n_{\mathbf{z}, \sigma} n_{\mathbf{x}, \sigma'} \rangle - \langle n_{\mathbf{z}, \sigma} \rangle \langle n_{\mathbf{x}, \sigma'} \rangle$ the correlated part of the density-density correlation function. To obtain these equations we have neglected next nearest neighbors hopping (details of the calculation in the Appendix). The solutions after a Fourier transform are given by:

$$\mathcal{G}_{\mathbf{k}, \mathbf{k}'}^{\alpha, \beta} = 2g_{\mathbf{k}+\mathbf{k}'}^{\beta, \beta} \frac{2\delta_{\alpha, \beta} |J_{\mathbf{k}}^{\alpha, \bar{\alpha}}|^2 - \delta_{\bar{\alpha}, \beta} J_{\mathbf{k}}^{\alpha, \beta} (\omega - \omega_{0, \beta})}{(\omega - \omega_{\mathbf{k}, +}) (\omega - \omega_{\mathbf{k}, -})} \quad (26)$$

$$\mathcal{G}_{\mathbf{k}, \mathbf{k}'}^{\sigma \sigma \alpha, \beta} = \delta_{\alpha, \beta} \frac{N \delta(\mathbf{k} + \mathbf{k}') \bar{n}_{\sigma} (1 - \bar{n}_{\sigma}) V_{\mathbf{k}'}^{\alpha, \sigma}}{\pi (\omega - \omega_{0, \alpha})^2} + \delta_{\alpha, \beta} \frac{\sum_{\sigma'} V_{\mathbf{k}'}^{\alpha, \sigma'} \langle n_{\mathbf{k}, \sigma} n_{\mathbf{k}', \sigma'} \rangle_C}{\pi (\omega - \omega_{0, \alpha})^2} \quad (27)$$

where the new poles of the Green's function $\mathcal{G}_{\mathbf{k}, \mathbf{k}'}^{\alpha, \beta}(\omega)$ are:

$$\omega_{\mathbf{k}, \pm} = \pm \tilde{\omega}_{\mathbf{k}} = \pm \sqrt{4 |J_{\mathbf{k}}^{-, +}|^2 + x^2 \delta V_0^2} \quad (28)$$

$V_0 = V_0^{+, +} + V_0^{-, +}$, $\delta V_0 = V_0^{+, +} - V_0^{-, +}$ and we have fixed $\mu = V_0$. Finally, we can characterize the diagonal Green's function including $1/\mathcal{Z}$ corrections (Eq.23):

$$G_{\mathbf{k}}^{\alpha, \beta} = g_{\mathbf{k}}^{\alpha, \beta} - \frac{2}{N} \sum_{\mathbf{q}} J_{\mathbf{q}}^{\alpha, \bar{\alpha}} \frac{\mathcal{G}_{\mathbf{q}, \mathbf{k}-\mathbf{q}}^{\bar{\alpha}, \beta}}{(\omega - \omega_{0, \alpha})} \quad (29)$$

$$- \frac{2J_1 g_{\mathbf{k}}^{\bar{\alpha}, \beta}}{(\omega - \omega_{0, \alpha})} + \frac{2}{N} \sum_{\sigma, \mathbf{q}} V_{\mathbf{q}}^{\alpha, \sigma} \frac{\mathcal{G}_{\mathbf{q}, \mathbf{k}-\mathbf{q}}^{\sigma \sigma \alpha, \beta}}{(\omega - \omega_{0, \alpha})}$$

Note that in general we should extract the value of the chemical potential from the self-consistency equations, once we have fixed the total number of particles. Instead we will prove that our choice is correct by checking with the self-consistency equation later on. Nevertheless, this is the expected value when next nearest neighbor hopping is neglected. The reason is that next nearest neighbor hopping shifts the conduction and valence band, breaking particle-hole symmetry. This implies that for half filling the chemical potential shifts from the neutral point. Then if $J_{\mathbf{k}}^{\alpha, \alpha}$ is neglected, particle-hole symmetry is recovered and the chemical potential is located between the bands.

As one can observe in Eq.29, the Green's function $G_{\mathbf{k}}^{\alpha, \beta}$ contains several new contributions: The first term corresponds to the uncorrelated solution previously found; the second term corresponds to the hybridization between sites due to the hopping and it is characterized by dispersive quasi-particle excitations; the third term only contributes for $\alpha \neq \beta$, and represents a hopping between two different sub-lattices, influenced by the density of particles in each of them; the last term corresponds to the effect of density-density correlations.

Self-consistency equations

We can use the previous expression for the 2-point function (Eq.29) to calculate the average number of particles in each sub-lattice:

$$\langle n_{\mathbf{x}, \alpha} \rangle^{\mathbf{k}} = i \int \frac{G_{\mathbf{k}}^{\alpha, \beta}(\omega + i\epsilon) - G_{\mathbf{k}}^{\alpha, \beta}(\omega - i\epsilon)}{e^{\beta\omega} + 1} d\omega \quad (30)$$

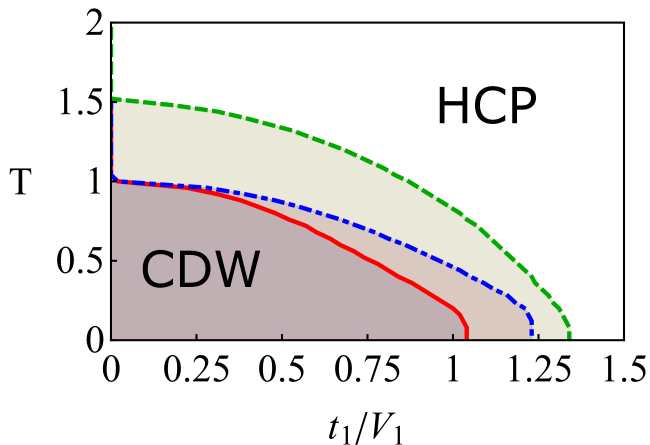


Figure 2: Phase diagram in absence of density-density correlations for the real space hierarchy. We find a HCP and a CDW phase as a function of t_1/V_1 . We plot the case of a honeycomb lattice (dashed green) and a dimerized chain in the topological ($\lambda = t'_1/t_1 = 1.25$, red) and trivial ($\lambda = 0.75$, blue) phase, for $V_2 = 0$. The addition of density-density correlations in the self-consistency equation shifts the critical point to $t_1/V_1 \rightarrow \infty$ (Fig.3).

In the Appendix we give details of the explicit calculation of the statistical average. The general result is:

$$\langle n_{\mathbf{x},\alpha} \rangle^{\mathbf{k}} = N\delta(\mathbf{k}) \left[\frac{1}{2} - \frac{1}{N} \sum_{\mathbf{q}} \frac{\omega_{0,\alpha}}{2\tilde{\omega}_{\mathbf{q}}} \tanh\left(\frac{\beta\tilde{\omega}_{\mathbf{q}}}{2}\right) \right] - N\delta(\mathbf{k}) \bar{n}_{\alpha} (1 - \bar{n}_{\alpha}) \sinh(\beta\omega_{0,\alpha}) \quad (31)$$

where the last term corresponds to the contribution from density-density correlations. It is clear from Eq.31 that our choice of the chemical potential ($\mu = V_0$) fulfills the self consistency equation for the number of particles at half filling $\sum_{\mathbf{y},\alpha} \langle f_{\mathbf{y},\alpha}^{\dagger} f_{\mathbf{y},\alpha} \rangle / N = 1$. In addition, the self-consistency equation for the asymmetry factor becomes:

$$x = -\frac{1}{N} \sum_{\mathbf{q}} \frac{x\delta V_0}{\tilde{\omega}_{\mathbf{q}}} \tanh\left(\frac{\beta\tilde{\omega}_{\mathbf{q}}}{2}\right) - \frac{1-x^2}{2} \sinh(\beta x \delta V_0) \quad (32)$$

Eq.32 shows two contributions: On one hand, the first term gives rise to a phase boundary between a homogeneous charge phase ($x = 0$) and a CDW phase with broken sub-lattice symmetry ($x \neq 0$), characteristic of the RPA approximation (Fig.2); the second term encodes the effect of density-density correlations, which favor the CDW phase and dominate at low temperature (Fig.3). Importantly, the symmetry broken phase only exists for the case $\delta V_0 = V_0^{+,+} - V_0^{+,-} < 0$, i.e., when nearest neighbors interaction V_1 dominates over next nearest neighbors V_2 . Note that the sum of both contributions give rise to the critical temperature found in the last section $T_c = \mathcal{Z}V_1$ (for $t_1 = 0$), but the $T = 0$ phase transition is lifted by the second term to $t_1/V_1 \rightarrow \infty$.

Therefore, density-density correlations stabilize the CDW phase, and hybridization only affects the finite

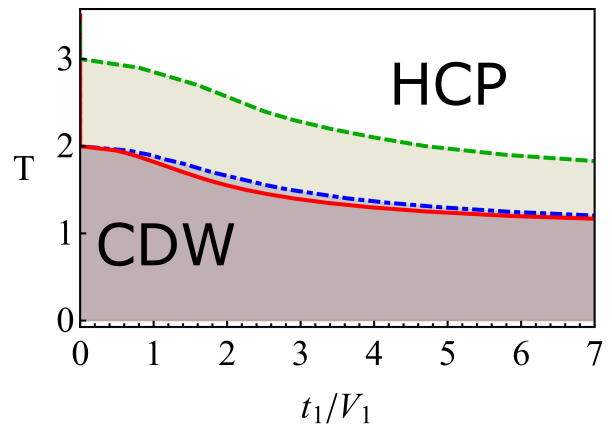


Figure 3: Full phase diagram for the real space hierarchy including density-density correlations ($V_2 = 0$). At $T = 0$ the CDW phase boundary extends to $t_1/V_1 \rightarrow \infty$, meaning that the HCP is only present in absence of interactions $V_1 = 0$, as previously found in absence of correlations. Hybridization only affects to the finite temperature region of the phase diagram, lowering the critical temperature from $T_c = \mathcal{Z}V_1$.

temperature phase boundary. However, in contrast with the uncorrelated case, the system now contains dispersive particle excitations (Eq.28) and the homogeneous charge phase is not equivalent to the Mott insulator, previously found in absence of correlations. For the case of the honeycomb lattice, the homogeneous charge phase describes a semi-metal with two Dirac cones.

We must comment that the finite temperature phase transitions in 1D are artifacts coming from the mean-field-like approach to lowest order, as in general the phase transitions should strictly exist at $T = 0$ only. Furthermore, the presence of a CDW phase for infinitesimal interaction goes against the results obtained from bosonization in 1D and well established results in the honeycomb lattice. For these reason we study in the next section an alternative form of the hierarchy for \mathbf{k} space correlations.

Finally, note that in the system with periodic boundary conditions, the case $\lambda > 1$ and $\lambda < 1$ must be connected by a translation. This can be easily seen from the self-consistency equation for x , but in Fig.2 one must perform a re-scaling $t_1 \leftrightarrow t'_1$ to confirm it.

IV. \mathbf{k} SPACE HIERARCHY

In this section we study the hierarchy for \mathbf{k} space correlations. Now the ground state is made of \mathbf{k} space modes $\{f_{\mathbf{k},\sigma}^{\dagger}, f_{\mathbf{k},\sigma}\}$ initially decoupled, and the non-local terms introduce correlations between them. If we Fourier transform Eq.5, we obtain the \mathbf{k} space representation of the Hamiltonian:

$$H = - \sum_{\mathbf{k}, \sigma, \sigma'} \left(J_{\mathbf{k}}^{\sigma, \sigma'} f_{\mathbf{k},\sigma}^{\dagger} f_{\mathbf{k},\sigma'} + \text{h.c.} \right) - \mu \sum_{\mathbf{k}, \sigma} n_{\mathbf{k},\sigma}$$

$$+\frac{1}{N} \sum_{\mathbf{q}} \sum_{\substack{\mathbf{k}, \mathbf{k}' \\ \sigma, \sigma'}} V_{\mathbf{q}}^{\sigma, \sigma'} f_{\mathbf{k}, \sigma}^{\dagger} f_{\mathbf{k}', \sigma'}^{\dagger} f_{\mathbf{k}' - \mathbf{q}, \sigma'} f_{\mathbf{k} + \mathbf{q}, \sigma} \quad (33)$$

where we have used:

$$f_{\mathbf{x}, \sigma}^{\dagger} = \frac{1}{\sqrt{N}} \sum_{\mathbf{k}} f_{\mathbf{k}, \sigma}^{\dagger} e^{i\mathbf{k} \cdot \mathbf{x}} \quad (34)$$

$$f_{\mathbf{x}, \sigma} = \frac{1}{\sqrt{N}} \sum_{\mathbf{k}} f_{\mathbf{k}, \sigma} e^{-i\mathbf{k} \cdot \mathbf{x}} \quad (35)$$

As for the real space hierarchy, we need to characterize the scaling properties of correlations in \mathbf{k} space, which in general will be different from the scaling of spatial correlations. We apply a similar analysis to the one used in the first section of this manuscript, studying the propagation of correlations for an excitation created with some initial momentum \mathbf{k} . However, let us first discuss some properties of Eq.33: One important difference with the real space representation (Eq.5) is that the hopping is now a local term (the momentum \mathbf{k} of an excitation does not change if we neglect particle interactions). Furthermore, the behavior of $V_{\mathbf{q}}$ as a function of \mathbf{q} is completely different from the one of $V_{\mathbf{x}}$ as a function of \mathbf{x} , which is a crucial change with respect to the real space hierarchy. The reason is that short range potentials become

long range in \mathbf{k} space. Then, we expect correlations to spread differently, and for some potentials, between a larger number of modes than in real space.

To define the scaling in a more precise way and study the system properties, we introduce the next 2-point function:

$$G_{\mathbf{k}}^{\alpha, \beta}(t, t') = -i \langle \langle f_{\mathbf{k}, \alpha}(t); f_{\mathbf{k}, \beta}^{\dagger}(t') \rangle \rangle \quad (36)$$

which characterizes the propagation of a particle with momentum \mathbf{k} from sub-lattice β to α . As in the previous section, we calculate the equation of motion:

$$(\omega + \mu) G_{\mathbf{k}}^{\alpha, \beta} = \frac{\delta_{\alpha, \beta}}{2\pi} - 2 \sum_{\sigma} J_{\mathbf{k}}^{\alpha, \sigma} G_{\mathbf{k}}^{\sigma, \beta} + \frac{2}{N} \sum_{\mathbf{k}_1, \mathbf{q}, \sigma} V_{\mathbf{q}}^{\alpha, \sigma} G_{\mathbf{k}_1, \mathbf{k}_1 - \mathbf{q}, \mathbf{k} + \mathbf{q}; \mathbf{k}}^{\sigma, \sigma, \alpha; \beta} \quad (37)$$

where we have defined the 4-point Green's function $G_{\mathbf{k}_1, \mathbf{k}_1 - \mathbf{q}, \mathbf{k} + \mathbf{q}; \mathbf{k}}^{\sigma, \sigma, \alpha; \beta} = -i \langle \langle f_{\mathbf{k}_1, \sigma}^{\dagger} f_{\mathbf{k}_1 - \mathbf{q}, \sigma} f_{\mathbf{k} + \mathbf{q}, \alpha}; f_{\mathbf{k}, \beta}^{\dagger} \rangle \rangle$. We see from Eq.37 that due to the \mathbf{q} dependence of $V_{\mathbf{q}}$, the analysis is more involved than in the real space hierarchy. Let us first expand to linear order in correlations the non-local term in Eq.37 (i.e., we include up to two point correlations):

$$\begin{aligned} \sum_{\mathbf{k}_1, \mathbf{q}} V_{\mathbf{q}}^{\alpha, \sigma} G_{\mathbf{k}_1, \mathbf{k}_1 - \mathbf{q}, \mathbf{k} + \mathbf{q}; \mathbf{k}}^{\sigma, \sigma, \alpha; \beta} &\simeq \sum_{\mathbf{k}_1} V_0^{\alpha, \sigma} \bar{n}_{\mathbf{k}_1, \sigma} G_{\mathbf{k}}^{\alpha, \beta} - \sum_{\mathbf{k}_1} V_{\mathbf{k}_1 - \mathbf{k}}^{\alpha, \sigma} \langle f_{\mathbf{k}_1, \sigma}^{\dagger} f_{\mathbf{k}_1, \alpha} \rangle G_{\mathbf{k}}^{\sigma, \beta} \\ &+ \sum_{\mathbf{k}_1} V_0^{\alpha, \sigma} \mathcal{G}_{\mathbf{k}_1, \mathbf{k}_1, \mathbf{k}; \mathbf{k}}^{\sigma, \sigma, \alpha; \beta} - \sum_{\mathbf{k}_1} V_{\mathbf{k}_1 - \mathbf{k}}^{\alpha, \sigma} \mathcal{G}_{\mathbf{k}_1, \mathbf{k}_1, \mathbf{k}; \mathbf{k}}^{\sigma, \alpha, \sigma; \beta} \end{aligned} \quad (38)$$

where we have neglected terms involving three or more points (this is not important as they are expected to be of higher order in the corresponding scaling parameter). Note that the two dominant contributions at this order are $\mathbf{q} = 0$ and $\mathbf{q} = \mathbf{k}_1 - \mathbf{k}$, which correspond to a direct and exchange channels, respectively. The first line of Eq.38 contains the uncorrelated contributions, while the second line the correlated ones.

We discuss the term proportional to $V_0^{\alpha, \sigma}$ first: We assume that the system is in a highly correlated state, which implies that $\mathcal{G}_{\mathbf{k}_1, \mathbf{k}_1, \mathbf{k}; \mathbf{k}}^{\sigma, \sigma, \alpha; \beta}$ has reached a maximum value as a function of $\rho_{\mathbf{k}_1, \mathbf{k}}^C$. If we include an additional particle to the lattice (i.e., an extra state in the sum), we find that due to the entanglement monogamy $\mathcal{G}_{\mathbf{k}_1, \mathbf{k}_1, \mathbf{k}; \mathbf{k}}^{\sigma, \sigma, \alpha; \beta}$ must decrease as $1/N_p$, being N_p the number of particles in the system. Therefore, the scaling of the non-local interaction term $V_{\mathbf{q}=0}^{\alpha, \sigma}$ must be proportional to $1/N_p$. Note that this only applies to correlations created by $V_0^{\alpha, \sigma}$, and in order to find a lower bound for the scaling, we

must analyze $V_{\mathbf{q} \neq 0}^{\alpha, \sigma}$ as well.

As the case with $\mathbf{q} \neq 0$ is more complicated, let us assume that the interaction potential $V_{\mathbf{q}}$ dominates for some $\mathbf{q}_0 = \mathbf{k}_1 - \mathbf{k} \neq 0$. Due to the nearest neighbors approximation used in the real space hierarchy, the interaction potential $V_{\mathbf{q}}$ is a periodic function of \mathbf{q} , i.e., $V_{\mathbf{q}_0} = V_{\mathbf{q}_0 + \mathbf{Q}}$ for some \mathbf{Q} vector in the Brillouin zone (BZ). The systems considered in this work are at half-filling and have sub-lattice symmetry, which implies that every \mathbf{k}_1 point couples to all other points in the BZ, as they are all occupied. Then for a large system we can rewrite the sum as $\sum_{\mathbf{k}_1} V_{\mathbf{k}_1 - \mathbf{k}}^{\alpha, \sigma} \mathcal{G}_{\mathbf{k}_1, \mathbf{k}_1, \mathbf{k}; \mathbf{k}}^{\sigma, \alpha, \sigma; \beta} = V_{\mathbf{q}_0}^{\alpha, \sigma} \sum_n \mathcal{G}_{\mathbf{k} + n\mathbf{Q}, \mathbf{k} + n\mathbf{Q}; \mathbf{k}; \mathbf{k}}^{\sigma, \alpha, \sigma; \beta}$ ($n \in \mathbb{Z}$), where n runs over a large number of values, that for simplicity, we approximate as being proportional to N_p (it will be smaller, but still a large number compared with \mathcal{Z} in the real space hierarchy). As previously, if we add a new state into the sum, the correlations between all previous particles must decrease as $n^{-1} \propto N_p^{-1}$. As we assumed that \mathbf{q}_0 was the dominant contribution, all other \mathbf{q} values should provide a better scaling, and we

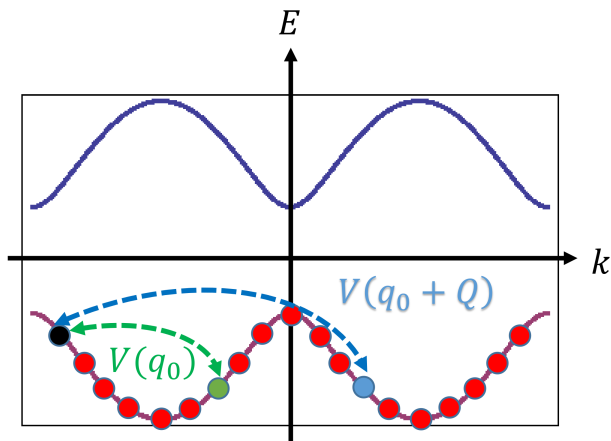


Figure 4: Correlations in \mathbf{k} space. An initial state with momentum \mathbf{k} interacts with all other particles in the system via the exchange of \mathbf{q} . If we assume for simplicity that some \mathbf{q}_0 dominates the interaction process, we show for a section of the BZ that different states can couple with the same $V_{\mathbf{q}_0} = V_{\mathbf{q}_0+n\mathbf{Q}}$, as $V_{\mathbf{q}}$ is a periodic function of \mathbf{q} . Then for a large system we find that $n \propto N_p$, and the scaling of the interaction term $V_{\mathbf{q}_0}$ must be proportional to N_p^{-1} .

can conclude that the lower bound is given by $V_{\mathbf{q}} \propto N_p^{-1}$ for all \mathbf{q} . In Fig.4 we illustrate the scaling properties of the interaction part of the Hamiltonian following the previous discussion. Note that the number of points connected with the same $V_{\mathbf{q}_0}$ correspond to the analog of the coordination number in the real space hierarchy, and strongly depend on the shape of the Brillouin zone and on the specific interaction potential. However, many typical interactions considered in many-body systems would give rise to a periodic $V_{\mathbf{q}}$, which provides a general improvement over the $1/Z$ scaling. More complicated interactions such as dipolar must be carefully analyzed to find if the scaling of spatial or \mathbf{k} space correlations is more efficient³⁹.

It is worth mentioning that the scaling of correlations in \mathbf{k} space is, in many cases, more efficient than the real space one, specially when we are dealing with low coordination numbers, as for the case of low dimensional systems. Nevertheless, as we will determine the self-consistency equations in this approach, we can directly compare the results of both hierarchies.

We stress that the general arguments given in this manuscript to estimate the scaling of correlations, rely on the assumption of having a fully correlated state. In more detailed calculation the precise scaling could be estimated in terms of direct calculations of entanglement between modes. However, the arguments used in this manuscript allow us to compare different hierarchies in a very systematic way, which is the purpose of this work.

A. Uncorrelated solution

We first obtain the uncorrelated solutions to Eq.37. If we make use of the scaling of the interaction term $V_{\mathbf{q}} \propto N_p^{-1}$, we find:

$$(\omega - \omega_{0,\alpha}) g_{\mathbf{k}}^{\alpha,\beta} = \frac{\delta_{\alpha,\beta}}{2\pi} - 2 \sum_{\sigma} J_{\mathbf{k}}^{\alpha,\sigma} g_{\mathbf{k}}^{\sigma,\beta} \quad (39)$$

where $\bar{n}_{\sigma} = \frac{1}{N} \sum_{\mathbf{k}_1} \bar{n}_{\mathbf{k}_1,\sigma}$ is the average number of particles in each sub-lattice. As the system of equations is diagonal in \mathbf{k} , the solution to the Green's function is easily obtained:

$$g_{\mathbf{k}}^{\alpha,\alpha} = \frac{\omega + \mu - 2 \sum_{\sigma} \bar{n}_{\sigma} V_0^{\bar{\alpha},\sigma}}{2\pi (\omega - \omega_{\mathbf{k},+}) (\omega - \omega_{\mathbf{k},-})} \quad (40)$$

$$g_{\mathbf{k}}^{\alpha,\bar{\alpha}} = \frac{-J_{\mathbf{k}}^{\alpha,\bar{\alpha}}}{\pi (\omega - \omega_{\mathbf{k},+}) (\omega - \omega_{\mathbf{k},-})} \quad (41)$$

where we have defined:

$$\omega_{\mathbf{k},\pm} = (\bar{n}_+ + \bar{n}_-) V_0 - \mu \pm \tilde{\omega}_{\mathbf{k}} \quad (42)$$

$$\tilde{\omega}_{\mathbf{k}} = \sqrt{x^2 \delta V_0^2 + 4 |J_{\mathbf{k},+}^-|^2} \quad (43)$$

and assumed nearest neighbors hopping only. Note that the Green's functions are the ones expected from the RPA approximation, and the quasi-particles are dispersive due to hybridization. The calculation of the average number of particles $\bar{n}_{\mathbf{k},\alpha}$ and average hybridization $\Delta_{\mathbf{k}}^{\bar{\alpha},\alpha}$ gives:

$$\bar{n}_{\mathbf{k},\alpha} = \frac{1}{2} - \alpha \frac{x \delta V_0}{2 \tilde{\omega}_{\mathbf{k}}} \tanh \left(\frac{\beta \tilde{\omega}_{\mathbf{k}}}{2} \right) \quad (44)$$

$$\langle f_{\mathbf{k},\bar{\alpha}}^{\dagger} f_{\mathbf{k},\alpha} \rangle_0 = \Delta_{\mathbf{k}}^{\bar{\alpha},\alpha} = \frac{J_{\mathbf{k}}^{\alpha,\bar{\alpha}}}{\tilde{\omega}_{\mathbf{k}}} \tanh \left(\frac{\beta \tilde{\omega}_{\mathbf{k}}}{2} \right) \quad (45)$$

Providing the next self-consistency equation for the asymmetry factor x :

$$x = -\frac{1}{N} \sum_{\mathbf{k}} \frac{x \delta V_0}{\tilde{\omega}_{\mathbf{k}}} \tanh \left(\frac{\beta \tilde{\omega}_{\mathbf{k}}}{2} \right) \quad (46)$$

where we have assumed half filling, and the chemical potential has been fixed to $\mu = V_0$, which allows to fulfill the self-consistency equation for the total number of particles, at arbitrary temperature. The phase diagram corresponds to the one shown in Fig.2, where the transition between the CDW and the homogeneous charge phase is controlled by the ratio $\delta V_0/t_1$. It is interesting that the self-consistency equation (Eq.46), corresponds to the one found in the real space hierarchy in absence of density-density correlations (Eq.32). Therefore in this case, the homogeneous charge phase is present for finite values of V_1 at $T = 0$, as shown in Fig.2. In addition, the critical temperature T_c is half the value that was found in the real space hierarchy. This result is in better agreement with the exact diagonalization and functional renormalization group studies^{24,28} (both on the honeycomb lattice), which confirms that the \mathbf{k} space hierarchy is more effective for the case of short ranged potentials.

B. Correlated solution

Here we include the effect of \mathbf{k} space correlations. We start from the full equation of motion for the 2-point

$$\begin{aligned}
 (\omega + \mu) G_{\mathbf{k}}^{\alpha,\beta} &= \frac{\delta_{\alpha,\beta}}{2\pi} - 2 \sum_{\sigma} J_{\mathbf{k}}^{\alpha,\sigma} G_{\mathbf{k}}^{\sigma,\beta} - \frac{2}{N} \sum_{\sigma, \mathbf{q} \neq 0} V_{\mathbf{q}}^{\sigma,\alpha} \langle f_{\mathbf{k}-\mathbf{q},\sigma}^{\dagger} f_{\mathbf{k}-\mathbf{q},\alpha} \rangle_0 g_{\mathbf{k}}^{\sigma,\beta} \\
 &+ \frac{2}{N} G_{\mathbf{k}}^{\alpha,\beta} \sum_{\sigma, \mathbf{k}_1} \bar{n}_{\mathbf{k}_1,\sigma} V_0^{\alpha,\sigma} + \frac{2}{N} \sum_{\sigma, \mathbf{k}_1 \neq \mathbf{k}} V_0^{\alpha,\sigma} \mathcal{G}_{\mathbf{k}_1, \mathbf{k}_1, \mathbf{k}; \mathbf{k}}^{\sigma, \sigma, \alpha; \beta}
 \end{aligned} \tag{47}$$

where we have separated the $\mathbf{q} = 0$ and $\mathbf{k}_1 = \mathbf{k} + \mathbf{q}$ terms in the sum, as they are the only ones that contribute to first order. We also neglected the contribution from $V_0^{\alpha,\sigma} g_{\mathbf{k}, \mathbf{k}, \mathbf{k}; \mathbf{k}}^{\sigma, \sigma, \alpha; \beta}$, which scales inversely proportional to the volume of the system. The contribution from the correlated part of the 4-point function $\mathcal{G}_{\mathbf{k}_1, \mathbf{k}_1, \mathbf{k}; \mathbf{k}}^{\sigma, \sigma, \alpha; \beta}$ can be obtained in a similar way to the previous section. We have calculated its equation of motion and found that in general, to first order, the correlated part of the density-density correlations $\langle n_{\mathbf{k},\alpha} n_{\mathbf{k}',\beta} \rangle_C$ can be neglected. Therefore the consequence of first order correlations in the equation of motion is the presence of response functions (convolutions) between the local statistical averages and the interaction potentials: $V_{\mathbf{k}}^{\sigma,\alpha} * \langle f_{\mathbf{k},\sigma}^{\dagger} f_{\mathbf{k},\alpha} \rangle_0 = \sum_{\mathbf{q}} V_{\mathbf{q}}^{\sigma,\alpha} \langle f_{\mathbf{k}-\mathbf{q},\sigma}^{\dagger} f_{\mathbf{k}-\mathbf{q},\alpha} \rangle_0 / N$.

We rewrite the equation of motion in the next compact form:

$$(\omega - \omega_{0,\alpha}) G_{\mathbf{k}}^{\alpha,\beta} = \frac{\delta_{\alpha,\beta}}{2\pi} - 2 \sum_{\sigma} J_{\mathbf{k}}^{\alpha,\sigma} G_{\mathbf{k}}^{\sigma,\beta} - 2\Lambda_{\mathbf{k}}^{\alpha,\beta} \tag{48}$$

where $\Lambda_{\mathbf{k}}^{\alpha,\beta} = \sum_{\sigma} g_{\mathbf{k}}^{\sigma,\beta} V_{\mathbf{k}}^{\sigma,\alpha} * \langle f_{\mathbf{k},\sigma}^{\dagger} f_{\mathbf{k},\alpha} \rangle_0$ corresponds to the response functions. The general solution to the system of equations is:

$$G_{\mathbf{k}}^{\alpha,\beta} = g_{\mathbf{k}}^{\alpha,\beta} + \frac{4J_{\mathbf{k}}^{\alpha,\bar{\alpha}} \Lambda_{\mathbf{k}}^{\bar{\alpha},\beta} - 2\Lambda_{\mathbf{k}}^{\alpha,\beta} (\omega - \omega_{0,\bar{\alpha}})}{(\omega - \omega_{\mathbf{k},+}) (\omega - \omega_{\mathbf{k},-})} \tag{49}$$

The Green's functions including correlations show the next interesting features:

- As $\Lambda_{\mathbf{k}}^{\alpha,\beta} \propto g_{\mathbf{k}}^{\sigma,\beta}$, the pole structure of the new contributions has order two poles. Naively one could think that this is the result from simple perturbation theory, however the presence of response functions proves otherwise. Furthermore, the presence of poles of order two is related to the fact that for the description of 2-point correlations we need pairs of excitations.
- The effect of correlations is encoded in the response functions $\Lambda_{\mathbf{k}}^{\alpha,\beta}$ and they represent the effect of interactions in the density distribution. As they are

Green's function (Eq.37), and include terms of order N_p^{-1} . We find:

present in the numerator, they modify the polynomial structure of the Green's functions allowing for the appearance of zeros. This will be related with the topological properties in the next section.

Self-consistency equations

In this section we first write explicit expressions for the response functions, and then we characterize the self-consistency equations including correlations. We first assume that the chemical potential is unchanged when correlations are included (this will be confirmed by direct calculation of the self-consistency equation for the number of particles), then we have $\mu = V_0^{+,+} + V_0^{-,+}$ for $J_{\mathbf{k}}^{\alpha,\alpha} = 0$. The expressions for the convolutions show that in this case, we have the next relation between them:

$$\begin{aligned}
 \chi_{\mathbf{k}}^{+,+} &= -x \frac{\delta V_0}{2N} \sum_{\mathbf{q}} \frac{V_{\mathbf{q}}^{+,+}}{\tilde{\omega}_{\mathbf{k}-\mathbf{q}}} \tanh\left(\frac{\beta \tilde{\omega}_{\mathbf{k}-\mathbf{q}}}{2}\right) \\
 &= -\chi_{\mathbf{k}}^{-,-}
 \end{aligned} \tag{50}$$

$$\begin{aligned}
 \chi_{\mathbf{k}}^{-,+} &= \frac{1}{N} \sum_{\mathbf{q}} V_{\mathbf{q}}^{-,+} \frac{J_{\mathbf{k}-\mathbf{q}}^{+,-}}{\tilde{\omega}_{\mathbf{k}-\mathbf{q}}} \tanh\left(\frac{\beta \tilde{\omega}_{\mathbf{k}-\mathbf{q}}}{2}\right) \\
 &= (\chi_{\mathbf{k}}^{+,-})^*
 \end{aligned} \tag{51}$$

where we have used the expressions for the uncorrelated statistical averages previously found, and the shorthand notation for the convolutions $\chi_{\mathbf{k}}^{\sigma,\alpha} = V_{\mathbf{k}}^{\sigma,\alpha} * \langle f_{\mathbf{k},\sigma}^{\dagger} f_{\mathbf{k},\alpha} \rangle_0$. Therefore, there are just two independent response functions. The calculation of the statistical averages is now straight forward, as the Green's functions highly simplify for our choice of the chemical potential:

$$G_{\mathbf{k}}^{\alpha,\beta} = g_{\mathbf{k}}^{\alpha,\beta} + \frac{4J_{\mathbf{k}}^{\alpha,\bar{\alpha}} \Gamma_{\mathbf{k}}^{\bar{\alpha},\beta} - 2\Gamma_{\mathbf{k}}^{\alpha,\beta} (\omega + \alpha x \delta V_0)}{(\omega - \omega_{\mathbf{k},+})^2 (\omega - \omega_{\mathbf{k},-})^2} \tag{52}$$

where $\Gamma_{\mathbf{k}}^{\alpha,\beta}$ corresponds to $\Lambda_{\mathbf{k}}^{\alpha,\beta}$ without the pole contribution. The expectation values including correlations are given by:

$$\langle n_{\mathbf{k},\pm} \rangle = \frac{1}{2} \pm \frac{2\chi_{\mathbf{k}}^{+,+} - x\delta V_0}{2\tilde{\omega}_{\mathbf{k}}} \tanh\left(\frac{\beta\tilde{\omega}_{\mathbf{k}}}{2}\right) \pm x\delta V_0 \frac{J_{\mathbf{k}}^{-,+}\chi_{\mathbf{k}}^{-,+} + J_{\mathbf{k}}^{+,-}\chi_{\mathbf{k}}^{+,-} - x\delta V_0\chi_{\mathbf{k}}^{+,+}}{\omega_{\mathbf{k}}^2} \left[\frac{1}{\omega_{\mathbf{k}}} \tanh\left(\frac{\beta\omega_{\mathbf{k}}}{2}\right) - \frac{\beta}{2} \operatorname{sech}^2\left(\frac{\beta\omega_{\mathbf{k}}}{2}\right) \right] \quad (53)$$

It is clear from Eq.53 that the self-consistency equation for the number of particles is fulfilled when $\mu = V_0^{+,+} + V_0^{-,+}$, which confirms our choice for the chemical potential. In addition, the asymmetry factor is obtained from the next self-consistency equation:

$$x = \frac{1}{N} \sum_{\mathbf{k}} \frac{2\chi_{\mathbf{k}}^{+,+} - x\delta V_0}{\tilde{\omega}_{\mathbf{k}}} \tanh\left(\frac{\beta\tilde{\omega}_{\mathbf{k}}}{2}\right) + 2x\delta V_0 \frac{1}{N} \sum_{\mathbf{k}} \frac{x\delta V_0\chi_{\mathbf{k}}^{+,+} - J_{\mathbf{k}}^{+,-}\chi_{\mathbf{k}}^{+,-} - J_{\mathbf{k}}^{-,+}\chi_{\mathbf{k}}^{-,+}}{\tilde{\omega}_{\mathbf{k}}^2} \left[\frac{\beta}{2} \operatorname{sech}^2\left(\frac{\beta\tilde{\omega}_{\mathbf{k}}}{2}\right) - \frac{1}{\tilde{\omega}_{\mathbf{k}}} \tanh\left(\frac{\beta\tilde{\omega}_{\mathbf{k}}}{2}\right) \right] \quad (54)$$

The solution to Eq.54 provides the phase diagram. In Fig.5 we show this phase diagram for the case of a dimerized chain. The comparison between the uncorrelated and correlated phase boundaries show an interesting feature: For the case $\lambda = t'_1/t_1 < 1$ the homogeneous charge phase is stabilized by correlations, however for the case $\lambda > 1$ the CDW phase is the one stabilized. Furthermore, the case $\lambda < 1$ shows two inequivalent solutions $x \neq 0$ with different particle distributions, in contrast with the case $\lambda > 1$ with only one. As we will discuss in the next section, each choice of λ corresponds to a different topological phase.

In Fig.6 we compare the phase diagram for the honeycomb lattice with and without correlations. It shows that the semi-metallic phase becomes stabilized by 2-point correlations, shifting the critical point to larger interactions.

It is interesting to notice that the effect of correlations decreases as the dimensionality of the system increases, i.e., the correction to the uncorrelated solution is more pronounced for the case of a dimerized chain than for the honeycomb lattice. This is in agreement with what one would expect from the critical behavior of low dimensional systems, where quantum corrections should become more important as the system decreases its dimensionality.

V. TOPOLOGICAL PROPERTIES

One of the most interesting aspects of a non-perturbative approach is to ask whether some effects, which are genuinely non-perturbative, can be captured. Here we study topological phases which lie out of the non-interacting classification using the hierarchy of correlations, and demonstrate that this approach provides an efficient method to shed light on these elusive states of matter.

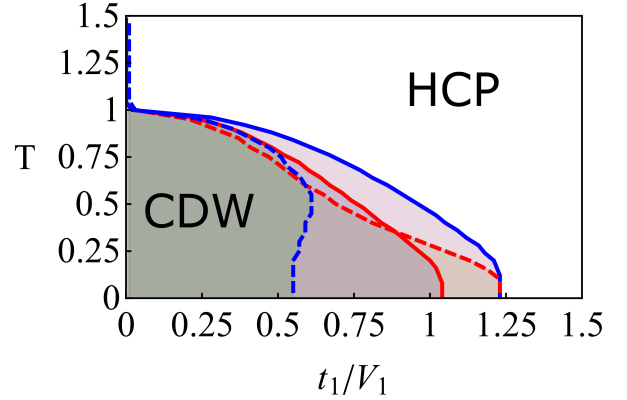


Figure 5: Phase diagram for the dimerized chain with nearest neighbors hopping and interaction ($V_2 = 0$). We have chosen $\lambda = 1.25$ and 0.75 (red and blue color, respectively). The continuous lines correspond to the uncorrelated case, while the dashed lines correspond to the one including 2-point correlations. It is interesting to see how correlations play an opposite role in the stabilization of the different phases. While the HCP is stabilized for the case $\lambda < 1$ (blue), the CDW phase is stabilized for $\lambda > 1$ (red). The $T = 0$ critical points shift to different values due to correlations, however the critical temperature remains unchanged. It is interesting to see that the correlated phase diagram for the case $\lambda < 1$ case shows a bump near $T \simeq 0.4$, where the CDW is stable for larger ratio t_1/V_1 than at the critical point.

A fundamental object in the characterization of the topological properties is the 2-point Green's function $G_{\mathbf{k}}^{\alpha,\beta}(t, t')$, which classifies mappings from the Brillouin zone to the space of n -dimensional matrices²⁹. This is a very natural way of classifying interacting topological phases, as in contrast with the use of the Hamiltonian, the Green's function contains information about symmetry broken phases and collective excitations. The Green's function has been used for the characterization of edge

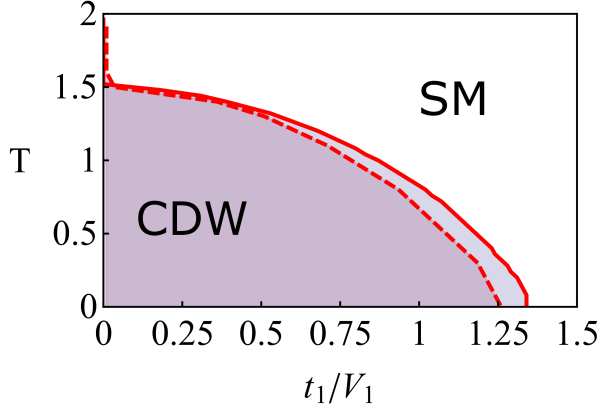


Figure 6: Phase diagram for the honeycomb lattice ($V_2 = 0$). The continuous line corresponds to the phase boundary between the CDW and the semi-metallic phase, when correlations are neglected. The dashed line corresponds to the case including correlations. The shift in the critical point towards a smaller value of t_1/V_1 means that the semi-metallic phase is stabilized by interactions.

states as well³⁰, and provides a new point of view on how interactions can affect the topological properties. One of the main consequences of this approach has been to show that interacting systems can exhibit zeros in the Green's function, and they play a similar role to poles (contributing to the topological index)^{31–33}. Therefore, the interacting topological phase turns out to be defined in terms of the poles and the zeros.

In this section we consider the full expression for the Green's function when 2-point correlations are included (Eq.49), and analyze the topological properties of the dimerized chain. We consider a dimerized chain due to its simplicity, and to the advantage that it has been thoroughly analyzed in previous works. It must be mentioned that the expression used in this manuscript for the winding number ν_1 could breakdown if the Green's function has branch cuts in the complex plane, instead of poles. Nevertheless, the models discussed in this work do not seem to exhibit these properties and our description should be correct.

In absence of interactions, the dimerized chain is characterized by a 1D winding number classifying maps from the Brillouin zone (\mathcal{S}^1) to the set of Hamiltonians with chiral symmetry (\mathcal{S}^1): $k \rightarrow \hat{H}_k$. If we consider just nearest neighbors, the winding number only depends on the ratio between the inter-dimer and the intra-dimer hopping $\lambda = t'_1/t_1$. When $\lambda > 1$, the winding number $\nu_1 = 1$ and the system is in a topological phase that shows localized edge states for open boundary conditions. On the other hand, when $\lambda < 1$ the winding number vanishes and the system does not exhibit edge states. Importantly, as

we have considered nearest neighbors only, the winding number cannot be larger than $\nu_1 = 1$.

When interactions are included, the effects of correlations are encoded in the Green's function. As previous works have shown, the 1D winding number can be written in terms of $G_k^{\alpha,\beta}$, and in absence of interactions, one recovers the well known expression in terms of the Hamiltonian. The maps characterized by the winding number correspond to $k \rightarrow \hat{G}_k$, where \hat{G}_k is the matrix with entries $G_k^{\alpha,\beta}$. Importantly, in the presence of interactions we will show that \hat{G}_k can lack of chiral symmetry, as there are contributions to the diagonal elements which are proportional to the asymmetry factor x when sub-lattice symmetry is spontaneously broken. This feature contrasts with the fact that the Hamiltonian of the system contains chiral symmetry (given as the product of time reversal and particle hole symmetry). This means that the Green's function is clearly more appropriate for the topological characterization than the Hamiltonian, as it contains more information about the system. Concretely, when the system is in the charge homogeneous phase ($x = 0$) of Fig.5, the Green's functions have chiral symmetry and the topological invariant must be given by the winding number ν_1 . In contrast, for the CDW phase ($x \neq 0$) we have to classify mappings from the circle to the sphere: $\mathcal{S}^1 \rightarrow \mathcal{S}^2$, and as they are always trivial, we always remain in a non-topological phase. In conclusion, for the dimerized chain we only need to pay attention to homogeneous charge phases, as they are the ones which can have a non-vanishing topological invariant.

Finally, let us mention that we can use $\hat{G}_k(\omega = 0)$, rather than the full Green's function $\hat{G}_k(\omega)$ for the calculation of the winding number, as they both contain the same topological properties in equilibrium³⁴. This feature allows us to highly improve the numerical calculation.

The Green's functions at $\omega = 0$ required for the characterization are:

$$G_k^{\alpha,\beta}(0) = g_k^{\alpha,\beta}(0) - \frac{4J_k^{\alpha,\bar{\alpha}}\Lambda_k^{\bar{\alpha},\beta}(0) - 2\alpha x \delta V_0 \Lambda_k^{\alpha,\beta}(0)}{\tilde{\omega}_k^2} \quad (55)$$

where $\Lambda_k^{\alpha,\beta}(\omega) \equiv \sum_{\sigma} g_k^{\sigma,\beta}(\omega) \chi_k^{\sigma,\alpha}$. Furthermore, if we particularize to homogeneous charge phases ($x = 0$), they simplify to:

$$G_k^{\alpha,\alpha}(0) = 0, \quad G_k^{\alpha,\bar{\alpha}}(0) = \frac{J_k^{\alpha,\bar{\alpha}}}{\pi \tilde{\omega}_k^2} \left(1 - \frac{\chi_k^{\alpha,\bar{\alpha}}}{J_k^{\bar{\alpha},\alpha}} \right) \quad (56)$$

and the matrix Green's function \hat{G}_k , whose entries are the Green's function with different sub-lattice indices, has the following general form:

$$\hat{G}_k(0) = \frac{1}{4\pi |J_k^{-,+}|^2} \begin{pmatrix} 0 & J_k^{+,-} \left(1 - \frac{\chi_k^{+,-}}{J_k^{-,+}}\right) \\ J_k^{-,+} \left(1 - \frac{\chi_k^{-,+}}{J_k^{+,-}}\right) & 0 \end{pmatrix} \quad (57)$$

where we know that the two response functions are related according to $\chi_k^{-,+} = (\chi_k^{+,-})^*$. This matrix clearly has chiral symmetry, implemented by $\mathcal{C} = \sigma_z$. Furthermore, we can see in Eq.57 that the contributions from the uncorrelated Green's function and the corrections due to correlations are clearly separated. Then, any change with respect to the winding number of the non-interacting system must come from the response functions. Finally, we

just need to apply the general expression for the winding number in terms of the Green's function^{34,35}:

$$\nu_1 = \frac{1}{4\pi i} \text{Tr} \oint \mathcal{C} \hat{G}_k^{-1} \partial_k \hat{G}_k dk \quad (58)$$

When we make use of Eq.57, we find:

$$\begin{aligned} \nu_1 = & \frac{1}{4\pi i} \oint \left(\frac{\partial_k J_k^{-,+}}{J_k^{-,+} - \chi_k^{+,-}} - \frac{\partial_k J_k^{+,-}}{J_k^{+,-} - \chi_k^{-,+}} \right) dk \\ & + \frac{1}{4\pi i} \oint \left(\frac{2\chi_k^{-,+} \partial_k J_k^{+,-} - J_k^{+,-} \partial_k \chi_k^{-,+}}{J_k^{+,-} (J_k^{+,-} - \chi_k^{-,+})} - \frac{2\chi_k^{+,-} \partial_k J_k^{-,+} - J_k^{-,+} \partial_k \chi_k^{+,-}}{J_k^{-,+} (J_k^{-,+} - \chi_k^{+,-})} \right) dk \end{aligned} \quad (59)$$

This equation shows that the winding number in presence of 2-point correlations has extra contributions encoded in the response functions. Furthermore, the corrections are proportional to the convolutions of the hybridization $\Delta_k^{\pm,\mp}$ with the interaction potential $V_k^{\pm,\mp}$. Therefore, when the system is in the homogeneous charge phase, the Green's function has chiral symmetry and the topological invariant is generally given by Eq.59. Furthermore, as this is a non-perturbative expression, it can be used for arbitrary values of the interaction potential. We plot in Fig.7 the change in the topological index ν_1 , as a function of the ratio between the hopping and the interaction strength t_1/V_1 .

It can be seen that the winding number changes with respect to the non-interacting case as a function of the interaction strength, for both the trivial ($t'_1/t_1 < 1$) and the topological phase ($t'_1/t_1 > 1$). More importantly, the winding number can reach values larger than one, which is not possible for the dimerized chain in absence of interactions. This is consistent with previous works where the value of the winding number is expected to change by unity²⁹.

It is important to note that for the calculation of the winding number we have assumed the homogeneous charge phase. Then one must compare the phase diagram with the one in Fig.5. This comparison shows that we would not be able to detect the change in the topological invariant when $t'_1 > t_1$ (the topological phase in the non-interacting case), as the CDW phase would dominate. However, it is interesting to see that the op-

posite would happen for the trivial phase: In the absence of interactions and for $t'_1 < t_1$ the system is a normal insulator. Then, when interactions reach a critical value $t_1/V_1 \simeq 2.2$, the insulator becomes topological with winding number $\nu_1 = -1$. As in the phase diagram of Fig.5, correlations stabilize the homogeneous phase to $t_1/V_1 \simeq 0.55$, the topological phase would exist for a wide range of the phase diagram.

We comment on one interesting aspect of the system behavior. The pole structure of the Green's function has not been changed when correlations are included, and one could think that the "band structure" of the system did not close the gap during the topological transition (this is a common feature of non-interacting topological insulators, where the only way to change a topological index is by closing the gap). Interestingly, in the presence of interactions the band structure is not enough to characterize the topological properties. As has been shown previously, the presence of interactions in the system introduces zeros in the Green's function and they can compete with the poles. These zeros are signatures of non-perturbative behavior^{29,33,36} and can annihilate the poles contribution, driving a topological phase into a trivial one. More importantly, the zeros are not linked to a gap closure, which means that we can have topological transitions without closing the gap.

Here we prove that the change in the topological invariant ν_1 is fully controlled by the appearance of zeros in $\hat{G}_k(\omega)$, as has been discussed in previous works. To track their appearance we calculate the determinant of

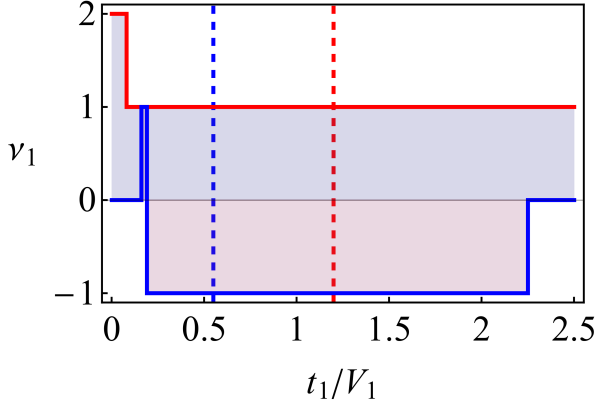


Figure 7: Winding number ν_1 of a dimerized chain as a function of t_1/V_1 for different ratios of the hopping $\lambda \in \{0.75, 1.25\}$ (blue and red, respectively). For large t_1/V_1 we recover the non-interacting winding number, and as interactions increase, the winding number changes. The topological phase (red) changes its winding number to $\nu_1 = 2$ when $t_1/V_1 \simeq 0.1$, and the trivial phase (blue) changes to $\nu_1 = -1$ at $t_1/V_1 \simeq 2.2$, and to $\nu_1 = 0$ at $t_1/V_1 \simeq 1.15$. The vertical dashed lines indicate the transition to the CDW phase from Fig.5. This calculation is performed assuming $T = 0$.

$\hat{G}_k(\omega)$ for the case of the homogeneous charge phase:

$$\det \hat{G}_k(\omega) = \frac{\omega^2 - 4(J_k^{-,+} - \chi_k^{+,-})(J_k^{+,-} - \chi_k^{-,+})}{4\pi^2(\omega^2 - 4|J_k^{-,+}|^2)^2} \quad (60)$$

From this expression one can see that zeros ω_z and poles ω_p appear for:

$$\omega_z = \pm 2\sqrt{(J_k^{-,+} - \chi_k^{+,-})(J_k^{+,-} - \chi_k^{-,+})} \quad (61)$$

$$\omega_p = \pm 2|J_k^{-,+}| \quad (62)$$

As the only quantity that depends on the interaction strength is ω_z , all topological changes should be linked to zeros of ω_z . In Fig.8 we plot ω_z as a function of t_1/V_1 , and confirm that all changes in the winding number correspond to zeros of the Green's function.

Furthermore, even the small region around $t_1/V_1 \sim 0.17$ in Fig.7, where the winding number changes from $\nu_1 = -1$ to $\nu_1 = 1$ for the case $t_1/t'_1 = 1.25$, is reflected in the behavior of the zeros (see Fig.9).

These results show that the topological characterization of strongly correlated systems can be very different from the characterization of non-interacting ones. This is due to the effect of correlations, which can make the quasi-particle picture to be insufficient due to the presence of collective excitations (now described by correlated excitations). Nevertheless, the use of Green's functions and of non-perturbative methods can be used to derive general results and capture the mechanisms driving topological transitions. Furthermore, the calculation of the motion of the zeros of the Green's function can be used

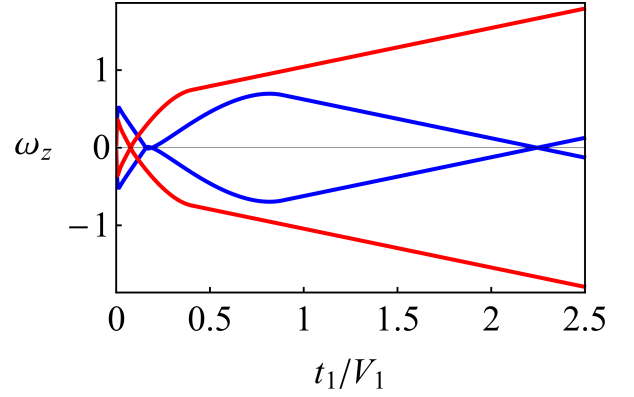


Figure 8: Evolution of zeros of $\hat{G}_k(\omega)$ as a function of t_1/V_1 . The blue(red) line corresponds to the ratio $t_1/t'_1 = 0.75$ (1.25). Note that all changes in the topological invariant correspond to zeros of the Green's function.

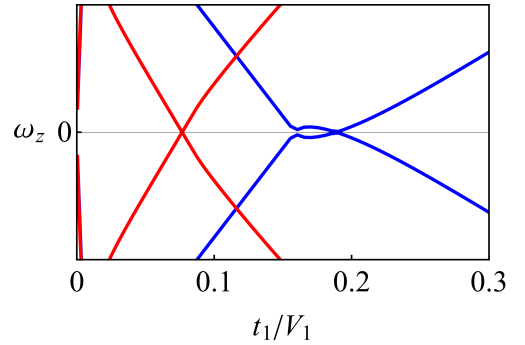


Figure 9: Zoom of Fig.8 to small t_1/V_1 . It shows that even the fast change in the winding number from $\nu_1 = -1$ to $\nu_1 = 1$ is captured by the zeros of the Green's function.

as a complementary “effective band structure” to keep track of topological changes.

It must be mentioned that the presence of the $\nu_1 = -1$ phase for the dimerized chain at intermediate coupling ($t_1 \sim V_1$) is surprising, as it has not been predicted previously. Its appearance corresponds to a regime away from both strong and weak coupling, and one must be careful to confirm that higher corrections due to correlations do not destroy this phase. In a future work we will address the numerical detection of this phase using alternative methods.

VI. CONCLUSIONS

In this work we have shown that a hierarchy of correlations can be a useful tool in the study of many-body systems. We have shown its connection with the $1/Z$ expansion, and generalized it to \mathbf{k} space correlations, being the basic ingredient the entanglement monogamy for strongly correlated systems. Although this method is very general, here we focused on interacting spinless particles in

a dimerized chain, and in a honeycomb lattice. In general \mathbf{k} space correlations scale differently from real space correlations, and we have proved that the former can be more efficient, concretely in systems with low coordination number. The results show that, for the honeycomb lattice, correlations tend to stabilize the semi-metallic phase, while correlations in the dimerized chain stabilize different phases depending on the ratio between the intra-dimer and the inter-dimer hopping (t'_1/t_1). Finally, we have studied how this approach can be applied to the study of topological phases with interactions. One of the advantages is the simplicity of the expressions when 2-point correlations are included, which provide information about the mechanisms that can cause a change in

the topological index when interactions are present. Furthermore, we have shown that the Green's functions in presence of correlations can have zeros, and that they are responsible for these topological changes.

Future extensions of this work will address the role of higher order correlations, the presence of long range interactions and non-equilibrium systems. Furthermore, it would be interesting to understand the relation between this approach and the renormalization group methods.

We would like to acknowledge F. Queisser, A. G. Grushin and P.C.E. Stamp for useful comments and the critical reading of the manuscript. This work was supported by NSERC, CIFAR, and PITP.

-
- * Electronic address: agomez@phas.ubc.ca
- ¹ A. O. Gogolin, A. Nersisyan, and A. M. Tsvelik, Cambridge University Press (1998).
 - ² H. Aoki et al., Rev. Mod. Phys. **86**, 779 (2014).
 - ³ A. Georges, G. Kotliar, W. Krauth, and M. J. Rozenberg, Rev. Mod. Phys. **68**, 13 (1996).
 - ⁴ S. Sachdev, *Quantum Phase transitions*, Cambridge University Press, 2011.
 - ⁵ V. Ginzburg and L. Landau, Zh. Eksp. Teor. Fiz. **20**, 1064 (1950).
 - ⁶ K. G. Wilson, Rev. Mod. Phys. **55**, 583 (1983).
 - ⁷ B. A. Bernevig, T. L. Hughes, and S.-C. Zhang, Science **314**, 1757 (2006).
 - ⁸ M. Z. Hasan and C. L. Kane, Rev. Mod. Phys. **82**, 3045 (2010).
 - ⁹ A. P. Schnyder, S. Ryu, A. Furusaki, and A. W. W. Ludwig, Phys. Rev. B **78**, 195125 (2008).
 - ¹⁰ C. Wang, A. C. Potter, and T. Senthil, Science **343**, 629 (2014).
 - ¹¹ S. Raghu, X.-L. Qi, C. Honerkamp, and S.-C. Zhang, Phys. Rev. Lett. **100**, 156401 (2008).
 - ¹² M. Dzero, K. Sun, V. Galitski, and P. Coleman, Phys. Rev. Lett. **104**, 106408 (2010).
 - ¹³ T. Neupert, L. Santos, C. Chamon, and C. Mudry, Phys. Rev. Lett. **106**, 236804 (2011).
 - ¹⁴ N. Regnault and B. A. Bernevig, Phys. Rev. X **1**, 021014 (2011).
 - ¹⁵ A. G. Grushin, A. Gómez-León, and T. Neupert, Phys. Rev. Lett. **112**, 156801 (2014).
 - ¹⁶ J.-X. L. Zhao-Long Gu, Kai Li, Arxiv: **1512.05118** (2015).
 - ¹⁷ A. Dutta et al., *Quantum phase transitions in transverse field spin models: From statistical physics to quantum information*, Cambridge University Press, 2015.
 - ¹⁸ R. S. Fishman and S. H. Liu, Phys. Rev. B **40**, 11028 (1989).
 - ¹⁹ H. M. Rønnow et al., Phys. Rev. B **75**, 054426 (2007).
 - ²⁰ F. Queisser, K. V. Krutitsky, P. Navez, and R. Schützhold, Phys. Rev. A **89**, 033616 (2014).
 - ²¹ C. Weeks and M. Franz, Phys. Rev. B **81**, 085105 (2010).
 - ²² E. V. Castro et al., Phys. Rev. Lett. **107**, 106402 (2011).
 - ²³ D. D. Scherer, M. M. Scherer, and C. Honerkamp, Phys. Rev. B **92**, 155137 (2015).
 - ²⁴ S. Capponi and A. M. Läuchli, Phys. Rev. B **92**, 085146 (2015).
 - ²⁵ J. Motruk, A. G. Grushin, F. de Juan, and F. Pollmann, Phys. Rev. B **92**, 085147 (2015).
 - ²⁶ V. Coffman, J. Kundu, and W. K. Wootters, Phys. Rev. A **61**, 052306 (2000).
 - ²⁷ D. N. Zubarev, Soviet Physics Uspekhi **3**, 320 (1960).
 - ²⁸ D. D. Scherer, M. M. Scherer, and C. Honerkamp, Phys. Rev. B, **1** (2015).
 - ²⁹ V. Gurarie, Phys. Rev. B **83**, 085426 (2011).
 - ³⁰ A. M. Essin and V. Gurarie, Phys. Rev. B **84**, 125132 (2011).
 - ³¹ Y.-Z. You, Z. Wang, J. Oon, and C. Xu, Phys. Rev. B **90**, 060502 (2014).
 - ³² S. R. Manmana, A. M. Essin, R. M. Noack, and V. Gurarie, Phys. Rev. B **86**, 205119 (2012).
 - ³³ K. B. Dave, P. W. Phillips, and C. L. Kane, Phys. Rev. Lett. **110**, 090403 (2013).
 - ³⁴ Z. Wang and S.-C. Zhang, Phys. Rev. X **2**, 031008 (2012).
 - ³⁵ M. Silaev and G. Volovik, J. Low Temp. Phys. **161**, 460 (2010).
 - ³⁶ T. Yoshida, R. Peters, S. Fujimoto, and N. Kawakami, Phys. Rev. Lett. **112**, 196404 (2014).
 - ³⁷ A. Osterloh and R. Schützhold, Phys. Rev. B **91**, 125114 (2015).
 - ³⁸ We mention that while finalizing this manuscript we became aware of a work with an analysis of the relation between the $1/\mathcal{Z}$ and the entanglement monogamy in terms of concurrence³⁷. We find their results consistent with the intuitive arguments given in this work.
 - ³⁹ Importantly, note that for a system away from half-filling or without sub-lattice symmetry the analysis of the scaling properties of correlations is more complicated, as some \mathbf{k}_1 states will not be occupied. This implies that a more asymmetric distribution of correlations for different \mathbf{k} states will be favored.
-

Appendix A: Correlated part of the 4-point function

In this appendix we include details of the calculation of the correlated part of the 4-point function in the real space hierarchy $\mathcal{G}_{\mathbf{x}\mathbf{y};\mathbf{y}}^{\sigma\sigma\alpha;\beta}$.

The general equation of motion for the 4-point function is given by ($\mathbf{z} \neq \mathbf{y}$):

$$\begin{aligned}
(\omega + \mu) G_{\mathbf{z}\mathbf{y};\mathbf{y}}^{\gamma_1\gamma_2\alpha;\beta} &= \langle f_{\mathbf{z},\gamma_1}^\dagger f_{\mathbf{z},\gamma_2} \rangle \frac{\delta_{\alpha,\beta}}{2\pi} + 2 (V_{\mathbf{z},\mathbf{z}}^{\gamma_1,\gamma_2} - V_{\mathbf{z},\mathbf{z}}^{\gamma_2,\gamma_2}) G_{\mathbf{z}\mathbf{z};\mathbf{y}}^{\gamma_1\gamma_2\alpha;\beta} \\
&+ 2 \sum_{\mathbf{x},\sigma} (J_{\mathbf{z},\mathbf{x}}^{\gamma_1,\sigma} G_{\mathbf{x}\mathbf{z};\mathbf{y}}^{\sigma\gamma_2\alpha;\beta} - J_{\mathbf{z},\mathbf{x}}^{\gamma_2,\sigma} G_{\mathbf{z}\mathbf{x};\mathbf{y}}^{\gamma_1\sigma\alpha;\beta} - J_{\mathbf{y},\mathbf{x}}^{\alpha,\sigma} G_{\mathbf{z}\mathbf{z}\mathbf{x};\mathbf{y}}^{\gamma_1\gamma_2\sigma;\beta}) \\
&- 2 \sum_{\mathbf{x},\sigma} (V_{\mathbf{z},\mathbf{x}}^{\gamma_1,\sigma} - V_{\mathbf{z},\mathbf{x}}^{\gamma_2,\sigma} - V_{\mathbf{y},\mathbf{x}}^{\alpha,\sigma}) G_{\mathbf{z}\mathbf{z}\mathbf{x}\mathbf{y};\mathbf{y}}^{\gamma_1\gamma_2\sigma\sigma\alpha;\beta}
\end{aligned} \tag{A1}$$

note that the 4-point function depends on the 6-point function now. This reminds of the BBGKY hierarchy in statistical mechanics, and a comparison between the \mathcal{Z}^{-1} hierarchy and the BBGKY has been previously discussed in²⁰. The correlated part can be obtained by removing the uncorrelated one:

$$\mathcal{G}_{\mathbf{z}\mathbf{z};\mathbf{y}}^{\gamma_1\gamma_2\alpha;\beta} = G_{\mathbf{z}\mathbf{z};\mathbf{y}}^{\gamma_1\gamma_2\alpha;\beta} - \langle n_{\mathbf{z},\sigma} \rangle G_{\mathbf{y};\mathbf{y}}^{\alpha;\beta} \tag{A2}$$

$$\begin{aligned}
(\omega + \mu) \mathcal{G}_{\mathbf{z}\mathbf{z};\mathbf{y}}^{\gamma_1\gamma_2\alpha;\beta} &= 2 (V_{\mathbf{z},\mathbf{z}}^{\gamma_1,\gamma_2} - V_{\mathbf{z},\mathbf{z}}^{\gamma_2,\gamma_2}) G_{\mathbf{z}\mathbf{z};\mathbf{y}}^{\gamma_1\gamma_2\alpha;\beta} \\
&+ 2 \sum_{\mathbf{x},\sigma} (J_{\mathbf{z},\mathbf{x}}^{\gamma_1,\sigma} G_{\mathbf{x}\mathbf{z};\mathbf{y}}^{\sigma\gamma_2\alpha;\beta} - J_{\mathbf{z},\mathbf{x}}^{\gamma_2,\sigma} G_{\mathbf{z}\mathbf{x};\mathbf{y}}^{\gamma_1\sigma\alpha;\beta}) - 2 \sum_{\mathbf{x},\sigma} J_{\mathbf{y},\mathbf{x}}^{\alpha,\sigma} (G_{\mathbf{z}\mathbf{z}\mathbf{x};\mathbf{y}}^{\gamma_1\gamma_2\sigma;\beta} - \langle f_{\mathbf{z},\gamma_1}^\dagger f_{\mathbf{z},\gamma_2} \rangle G_{\mathbf{x};\mathbf{y}}^{\sigma;\beta}) \\
&- 2 \sum_{\mathbf{x},\sigma} (V_{\mathbf{z},\mathbf{x}}^{\gamma_1,\sigma} - V_{\mathbf{z},\mathbf{x}}^{\gamma_2,\sigma}) G_{\mathbf{z}\mathbf{z}\mathbf{x}\mathbf{y};\mathbf{y}}^{\gamma_1\gamma_2\sigma\sigma\alpha;\beta} + 2 \sum_{\mathbf{x},\sigma} V_{\mathbf{y},\mathbf{x}}^{\alpha,\sigma} (G_{\mathbf{z}\mathbf{z}\mathbf{x}\mathbf{y};\mathbf{y}}^{\gamma_1\gamma_2\sigma\sigma\alpha;\beta} - \langle f_{\mathbf{z},\gamma_1}^\dagger f_{\mathbf{z},\gamma_2} \rangle G_{\mathbf{x}\mathbf{x}\mathbf{y};\mathbf{y}}^{\sigma\sigma\alpha;\beta})
\end{aligned} \tag{A3}$$

which must be supplemented with the conservation law $i\partial_t \langle f_{\mathbf{z},\gamma_1}^\dagger f_{\mathbf{z},\gamma_2} \rangle = 0$. Using the expansion in correlations and keeping terms to $1/\mathcal{Z}$ order, we find:

$$(\omega - \omega_{0,\alpha}) \mathcal{G}_{\mathbf{z}\mathbf{z};\mathbf{y}}^{\sigma\sigma\alpha;\beta} = 2\bar{n}_\sigma (1 - \bar{n}_\sigma) g_{\mathbf{y};\mathbf{y}}^{\alpha;\beta} V_{\mathbf{y};\mathbf{z}}^{\alpha,\sigma} + 2g_{\mathbf{y};\mathbf{y}}^{\alpha;\beta} \sum_{\sigma', \mathbf{x} \neq \mathbf{y}, \mathbf{z}} V_{\mathbf{y};\mathbf{x}}^{\alpha,\sigma'} \langle n_{\mathbf{z},\sigma} n_{\mathbf{x},\sigma'} \rangle_C \tag{A4}$$

Using the correlated part of the 4-point function to characterize the density-density correlations, we find after a Fourier transformation:

$$\begin{aligned}
\langle n_{\mathbf{k},\sigma} n_{\mathbf{k}',\sigma'} \rangle_C &= -N\delta(\mathbf{k} + \mathbf{k}') \bar{n}_\sigma (1 - \bar{n}_\sigma) \frac{V_{\mathbf{k}'}^{\sigma',\sigma} - \frac{V_{\mathbf{k}'}^{\sigma',\sigma'} V_{\mathbf{k}'}^{\sigma',\sigma}}{\frac{\beta}{2} \operatorname{sech}^2\left(\frac{\beta\omega_{0,\sigma'}}{2}\right) + V_{\mathbf{k}'}^{\sigma',\sigma'}}}{\frac{1}{\frac{\beta}{2} \operatorname{sech}^2\left(\frac{\beta\omega_{0,\sigma'}}{2}\right)} + V_{\mathbf{k}'}^{\alpha,\alpha} - \frac{|V_{\mathbf{k}'}^{\sigma',\sigma'}|^2}{\frac{\beta}{2} \operatorname{sech}^2\left(\frac{\beta\omega_{0,\sigma'}}{2}\right) + V_{\mathbf{k}'}^{\sigma',\sigma'}}}
\end{aligned} \tag{A5}$$

$$= -N\delta(\mathbf{k} + \mathbf{k}') \bar{n}_\sigma (1 - \bar{n}_\sigma) \lambda_{\mathbf{k}}^{\sigma,\sigma'} \tag{A6}$$

Then, the statistical averages including correlations can be easily found:

$$\begin{aligned}
\langle n_{\mathbf{x},\alpha} \rangle^{\mathbf{k}} &= N\delta(\mathbf{k}) \left[\frac{1}{2} - \frac{1}{N} \sum_{\mathbf{q}} \frac{\omega_{0,\alpha}}{2\tilde{\omega}_{\mathbf{k}}} \tanh\left(\frac{\beta\tilde{\omega}_{\mathbf{k}}}{2}\right) \right] \\
&+ \delta(\mathbf{k}) 4\beta^2 \operatorname{csch}^3(\beta\omega_{0,\alpha}) \sinh^4\left(\frac{\beta\omega_{0,\alpha}}{2}\right) \sum_{\sigma,\mathbf{q}} |V_{\mathbf{q}}^{\alpha,\sigma}|^2 \bar{n}_\sigma (1 - \bar{n}_\sigma) \\
&+ 4\beta^2 \operatorname{csch}^3(\beta\omega_{0,\alpha}) \sinh^4\left(\frac{\beta\omega_{0,\alpha}}{2}\right) \frac{1}{N} \sum_{\mathbf{q},\sigma,\sigma'} V_{\mathbf{q}}^{\alpha,\sigma} V_{\mathbf{k}-\mathbf{q}}^{\alpha,\sigma'} \langle n_{\mathbf{q},\sigma} n_{\mathbf{k}-\mathbf{q},\sigma'} \rangle_C \\
&= N\delta(\mathbf{k}) \left[\frac{1}{2} - \frac{1}{N} \sum_{\mathbf{q}} \frac{\omega_{0,\alpha}}{2\tilde{\omega}_{\mathbf{k}}} \tanh\left(\frac{\beta\tilde{\omega}_{\mathbf{k}}}{2}\right) \right]
\end{aligned} \tag{A7}$$

$$\begin{aligned}
& +N\delta(\mathbf{k}) 4\beta^2 \text{csch}^3(\beta\omega_{0,\alpha}) \sinh^4\left(\frac{\beta\omega_{0,\alpha}}{2}\right) \sum_{\sigma} \bar{n}_{\sigma} (1 - \bar{n}_{\sigma}) \frac{1}{N} \sum_{\mathbf{q}} |V_{\mathbf{q}}^{\alpha,\sigma}|^2 (1 - \lambda_{\mathbf{q}}^{\sigma,\sigma}) \\
& -N\delta(\mathbf{k}) 4\beta^2 \text{csch}^3(\beta\omega_{0,\alpha}) \sinh^4\left(\frac{\beta\omega_{0,\alpha}}{2}\right) \sum_{\sigma} \bar{n}_{\sigma} (1 - \bar{n}_{\sigma}) \frac{1}{N} \sum_{\mathbf{q}} V_{\mathbf{q}}^{\alpha,\sigma} V_{\mathbf{q}}^{\bar{\sigma},\alpha} \lambda_{\mathbf{k}}^{\sigma,\bar{\sigma}}
\end{aligned}$$

Interestingly one can calculate the integrals over \mathbf{q} in the continuum limit for both, nearest and next nearest neighbors interaction in the dimerized chain and in the honeycomb lattice. The result is surprisingly simple and does not depend on the details of the lattice or dimension (only on the coordination number \mathcal{Z}):

$$\langle n_{\mathbf{x},\alpha} \rangle^{\mathbf{k}} = N\delta(\mathbf{k}) \left[\frac{1}{2} - \frac{1}{N} \sum_{\mathbf{q}} \frac{\omega_{0,\alpha}}{2\tilde{\omega}_{\mathbf{q}}} \tanh\left(\frac{\beta\tilde{\omega}_{\mathbf{q}}}{2}\right) \right] - N\delta(\mathbf{k}) \bar{n}_{\alpha} (1 - \bar{n}_{\alpha}) \sinh(\beta\omega_{0,\alpha}) \quad (\text{A8})$$
